Post-Quench Ductility Results for Zry-4 and M5
Oxidized at 1000˚C and 1100˚C

Y. Yan, T. Burtseva and M. Billone
January 31, 2004

Summary

Ring compression tests have been completed for Zry-4 and M5 samples oxidized to nominal ECR values of 5, 10, 15, 17 and 20% at 1000˚C and 1100˚C. The 25-mm-long samples were exposed individually to two-sided steam oxidation in the same test apparatus for the same test times, slow cooled to 800˚C and water-quenched. The test times corresponding to the nominal ECR values were calculated based on the Cathcart-Pawel (CP) weight gain correlation and a wall thickness of 0.57 mm (Zry-4). The wall thickness of the M5 tubing is 0.61 mm. Based on sample weight increase (normalized to the surface area), weight gain was determined and compared to Cathcart-Pawel predictions. As expected, good agreement was achieved among both alloys and the predictions for the 1100˚C samples, while significant differences in weight gain vs. time were observed for the 1000˚C samples. For the highest oxidation time (≈3400 s) at 1000˚C, the M5 weight gain was ≈36% less than that for Zry-4. These experimental weight gains, along with the sample thickness, were used to determine experimental ECR values.

Ring-compression samples (8-mm-long) were cut from the oxidized samples and tested in a Model 4505 Instron at room temperature and 2 mm/minute cross-head displacement rate. This rate corresponds to a diametral strain rate of 0.35%/s for the 9.50 mm-OD cladding. Load-displacement curves were analyzed by the offset-displacement method to determine plastic ductility. As-received (non-oxidized) samples were tested to verify that the effective stiffness for the load-displacement curves agrees with predictions for ring stiffness (≈1 kN/mm). It was also found that the permanent displacement of non-oxidized rings compressed to 2 mm was ≈1 mm based on direct post-test measurement and ≈1.2 mm based on the offset method. The tests for two highly oxidized samples were stopped after the first significant load drop leading to a single, very tight, through-wall crack over the length of the ring. The offset strains were 3.2% and 2.5% as compared to 1.2% and 2.1%, respectively, determined from direct measurement. Therefore, samples with ≤0.2 mm (≈2%) offset displacement are considered to be brittle. All alloys exhibited offset strains > 2% and were assessed as ductile. The 1000˚C results were interesting in that both alloys retained ≈3% ductility after oxidation for the same test time (≈3400 s), even though the measured ECR values were 22.4% (Zry-4) and 13.3% (M5). These results suggest that embrittlement correlates better with oxidation time at 1000˚C and CP-predicted ECR than with measured weight gain and measured ECR.

Metallographic, microhardness and hydrogen-content analyses were performed on the highest ECR samples. These data, along with physical examination of the compressed samples, proved very useful in supporting post-quench-ductility evaluation.

1. Introduction

The purpose of this program is to determine the post-quench ductility of advanced cladding alloys ZIRLO and M5, as compared to the post-quench ductility of Zry-4. While extensive literature data are available for traditional Zircaloy claddings (Zry-4 and Zry-2), relatively little data have been published for ZIRLO and M5. Also, the published data for advanced alloys were generated in different laboratories by very different methods. In this program, all samples are oxidized in the same apparatus at the same ramp rates, hold times, and cooling rates (slow-cooled to 800˚C and water-quenched). The 25-mm-long samples are exposed to two-sided steam oxidation prior to cooling. Also, the samples are compressed in the same Instron machine, and the load-displacement data are analyzed by a common method to determine ductility.

The Zry-4 and ZIRLO tubing (17×17 PWR) provided by Westinghouse has an outer diameter of 9.50 mm and a wall thickness of 0.57 mm. The M5 tubing (17×17 PWR) provided by Framatome has an outer diameter of 9.50 mm and a wall thickness of 0.61 mm. Table 1 summarizes the test matrix for oxidizing the samples prior to ring-compression, post-quench ductility testing. The times listed are the equivalent isothermal times at the test temperature to give Cathcart-Pawel (CP) calculated ECR values of 5, 10, 15, 17, and 20%, for an assumed wall thickness of 0.57 mm. Actual ECR values vary depending on the weight gain for each sample and the as-fabricated thickness of the sample.

Following oxidation and quench, 8-mm rings were cut from near the middle of the 25-mm-long samples. Ring compression tests were performed at room temperature at a displacement rate of 2 mm/min. The load-displacement curves were analyzed by the traditional offset-displacement method. The offset displacement, which is a measure of permanent displacement, was normalized to the outer diameter (9.50 mm) to give a nominal plastic hoop strain. Samples that exhibited offset strains >2% were considered to be ductile. To aid in the interpretation of the load-displacement curves, post-test samples were examined physically, additional limited-displacement tests were conducted, and selective characterization (metallography, microhardness, and hydrogen analysis) was performed.

2. Steam Oxidation and Quench

References 1-2 describe the apparatus used to oxidize and quench the samples, along with thermal, chemical and metallographic verification and validation test results. Tables 2-3 show the measured weight gain and measured vs. predicted ECR values for the 1000˚C and 1100˚C oxidation temperatures, respectively. Figures 1-2 show, respectively, the weight gain results for M5 and Zry-4 oxidized at 1000˚C and 1100˚C. The 1100˚C results indicate that weight gain kinetics for both alloys are comparable and in agreement with the Cathcart-Pawel correlation. As ECR is based on wall thickness, the M5 experimental values are 0.57/0.61 = 0.934 times smaller than the Zry-4 values for the same weight gain. The 1000˚C weight-gain results indicate that the M5 values are significantly smaller than the Zry-4 values for the same test times.

Table 1 Test Matrix for Oxidation of Samples for Post-Quench Ductility Tests. The times and ECR values listed correspond to those calculated using the Cathcart-Pawel weight gain correlation, a nominal wall thickness of 0.57 mm, and two-sided isothermal oxidation in steam. The relationship between ECR (%) and normalized weight gain (Δw in mg/cm^2) is ECR = 1.538 Δw for 0.57-mm-thick cladding.

Temperature °C	**ECR %**	**Equivalent Oxidation Time s**
1000	5	210
	10	841
	15	1892
	17	2430
	20	3364
1100	5	67
	10	266
	15	599
	17	769
	20	1065
1200	5	25
	10	99
	15	222
	17	285
	20	394
1260	5	14
	10	58
	15	130
	17	167
	20	231

Table 2 Weight Gain (Δw in mg/cm^2) and Measured ECR (%) Values for Zry-4 and M5 Oxidized in Steam at 1000°C. For Zry-4, ECR = 1.538 Δw, while for M5 ECR = 1.437 Δw because of its thicker wall (0.61 mm vs. 0.57 mm). Alloys were oxidized for the same ramp rate, hold time and cooldown rate for each nominal ECR value.

Cathcart-Pawel ECR, %	Material	Measured Weight Gain (Δw), mg/cm^2	Measured ECR, %
5	Zry-4	3.9	6.1
4.7	M5	3.0	4.3
10	Zry-4	7.2	11.0
9.3	M5	5.3	7.6
15	Zry-4	11.0	16.9
14.1	M5	7.4	10.7
17	Zry-4	12.5	19.3
16.0	M5	8.0	11.6
20	Zry-4	14.6	22.4
18.8	M5	9.2	13.3
20.7*	M5	8.6	12.4

*Post-quench confirmation test sample generated at an equivalent time of ≈4100 s; note that the weight gain decreased from 9.3 to 8.6 mg/cm^2 with the increase of 700 s in oxidation time. Both samples exhibited smooth, black oxide layers with no indication of spallation.

Table 3 Weight Gain (Δw in mg/cm^2) and Measured ECR (%) Values for Zry-4 and M5 Oxidized in Steam at 1100˚C. For Zry-4, ECR = 1.538 Δw, while for M5 ECR = 1.437 Δw because of its thicker wall (0.61 mm vs. 0.57 mm). Alloys were oxidized for the same ramp rate, hold time and cooldown rate for each nominal ECR value.

Cathcart-Pawel ECR, %	Material	Measured Weight Gain (Δw), mg/cm^2	Measured ECR, %
5	Zry-4	4.0	6.2
4.7	M5	3.2	4.6
10	Zry-4	7.1	10.9
9.3	M5	6.4	9.2
15	Zry-4	10.6	16.3
14.1	M5	9.6	13.8
17	Zry-4	11.7	18.0
16.0	M5	11.3	16.2
20	Zry-4	13.2	20.3
18.7	M5	13.3	19.1
20.4*	M5	14.3	20.6

*Additional M5 test sample prepared to confirm post-quench ductility at ≈20% ECR

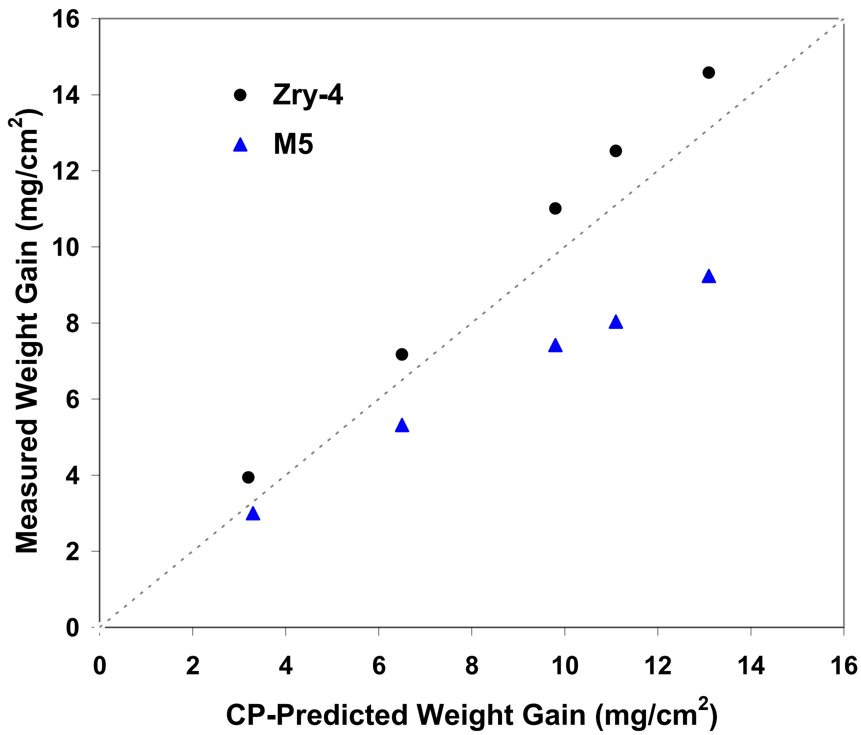

Fig. 1. Comparison between weight gain data for M5 and Zry-4 and weight gain predicted by the Cathcart-Pawel (CP) correlation for samples oxidized (two-sided) in steam at 1000˚C. Equivalent test times correspond to CP-calculated ECR values of 5, 10, 15, 17, and 20% for 0.57-mm-thick cladding (see Table 1).

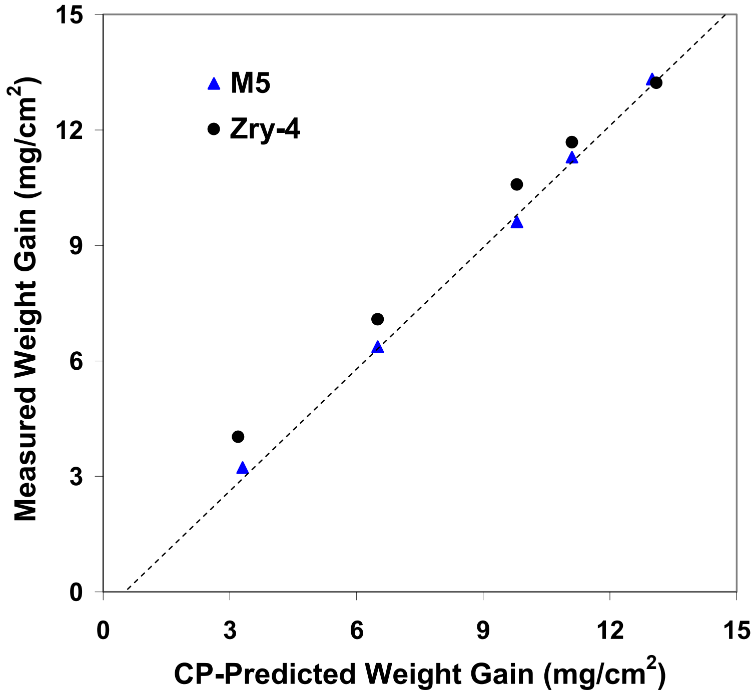

Fig. 2. Comparison between weight gain data for M5 and Zry-4 and weight gain predicted by the Cathcart-Pawel (CP) correlation for samples oxidized (two-sided) in steam at 1100˚C. Equivalent test times correspond to CP-calculated ECR values of 5, 10, 15, 17, and 20% for 0.57-mm-thick cladding (see Table 1).

3. Ring Compression Tests

3.1 Validation of Ring Compression Test and Data-Analysis Methodology

Ring compression tests were conducted at room temperature on 8-mm-long samples prepared from the central region of the 25-mm-long oxidized-and-quenched samples. Flat support and loading machine fixtures were used to compress the rings. Tests were conducted at a cross-head displacement rate of 2 mm/min. Normalizing this to the outer-diameter (9.50 mm) of the tubing gives a diametral strain rate of 0.35%/s. A Model 5566 table-top Instron machine had been ordered to conduct these tests. However, as there was a delay in delivery of this new Instron, the Model 4505 Instron, belonging to the ET Ceramics Section, was used. Initial tests were conducted on as-received tubing to compare the predicted ring elastic stiffness to the linearized slope of the load-displacement curve. The load-displacement curves gave an effective elastic stiffness of ≈1 kN/mm, which is in good agreement with the predicted value. Thus the machine stiffness is large relative to the sample stiffness. Additional ring-compression tests were conducted on validation samples of Zry-4 and M5, which had been oxidized and slow cooled without quench. A few validation samples, which had been subjected to quench, were also tested. "Ductility" was determined by the offset-displacement method used for interpretation of load-displacement curves for metals. Figure 3 shows the load-displacement curves for M5 validation samples oxidized to 17% ECR at 1100˚C and cooled without (Fig. 3a) and with (Fig. 3b) quench. The first significant load drop indicates a through-wall crack. The offset displacement method is illustrated on these curves. The method assumes that if the sample were unloaded just prior to cracking, it would unload with the same stiffness as the linearized portion of the initial load rise. This gives offset displacements of 0.559 mm for the unquenched sample and 0.610 mm for the quenched sample. Normalizing by the outer diameter to determine a nominal plastic hoop strain gives ≈6% offset strain for both cases, which implies that the samples are indeed ductile. A similar validation test was performed with a Zry-4 sample oxidized to 18% ECR and cooled without quench. The sample exhibited an offset strain of ≈4%. Hydrogen analysis and metallography were performed on this Zry-4 sample to support the conclusion that the sample should behave in a ductile manner from a materials perspective. The hydrogen pickup was low (8 wppm), indicating no hydrogen embrittlement. Also, the low-oxygen-containing prior-beta region, which is ductile, was effectively thick enough to support the ductility assessment based on the offset-displacement method.

In addition to the ring-compression validation tests with oxidized Zry-4 and M5, numerous tests were conducted on E110 cladding samples oxidized at 1100˚C (one-sided) and 1000˚C (two-sided) [3]. As this cladding embrittles at relatively low ECR values due to early breakaway oxidation and hydrogen pickup >200 wppm, the results were used to validate the determination of the ductile-to-brittle transition by means of the ring compression test. These ring-compression results vs. measured hydrogen content and calculated ECR are documented in a separate report for the E110 samples oxidized at 1000˚C [4].

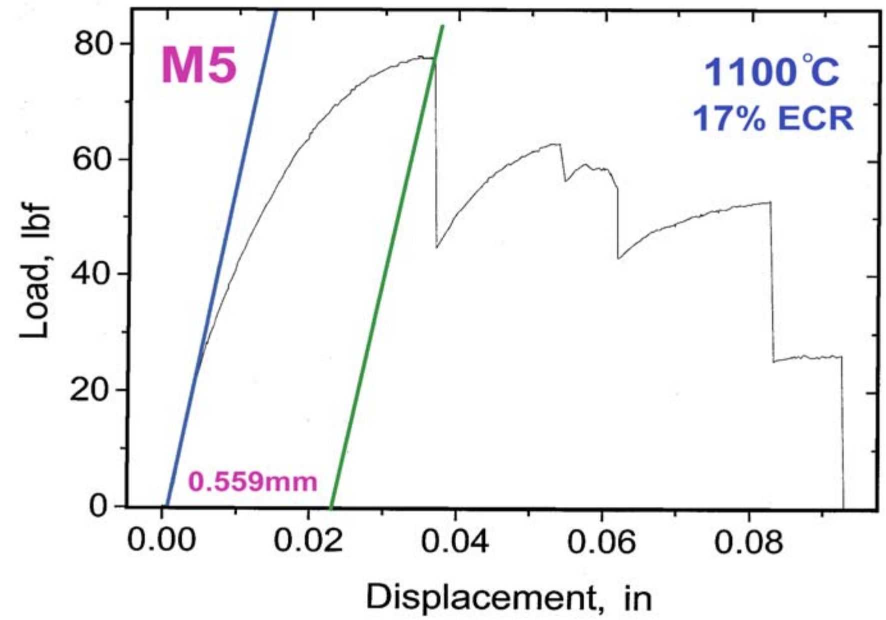

(a)

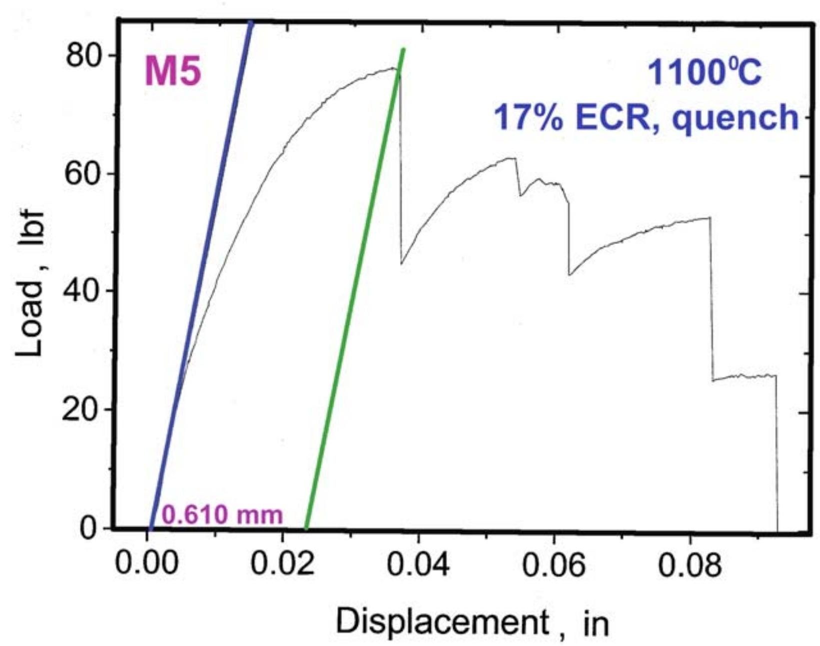

(b)

Fig. 3. Load-displacement curves for validation-lot M5 oxidized to 17% ECR without quench (a) and with quench (b) and compressed at 2 mm/min. at room temperature. The curves illustrate the offset displacement method used to determine plastic displacement. These displacements, normalized to the tubing diameter (9.5 mm), give a nominal plastic ductility of ≈6% in the hoop direction.

3.2 Post-Quench, Ring-Compression Data

From the samples listed in Tables 2 and 3, 8-mm-long rings were cut from the central region for ring-compression testing. As with the validation tests, these tests were conducted at room temperature and a cross-head displacement rate of 2 mm/min. The load-displacement curves from these tests are given in Appendix A for Zry-4 and in Appendix C for M5. Determination of offset displacement and strain for the 1000˚C and 1100˚C samples with the highest ECR values proved to be relatively straightforward. These samples exhibited four distinct load drops and broke into 4 pieces. The first significant load drop, which indicates through-wall failure, is very abrupt and occurs at relatively low displacement. However, at intermediate ECR values, it was often difficult to determine the load drop or decrease indicating failure. Cracking of the very brittle, high-oxygen alpha layers, as well as the brittle oxide layers, generates load drops that do not necessarily indicate through-wall failure. In order to interpret the load-displacement curves to determine offset strain, it was necessary to examine the intermediate-ECR samples to determine if indeed a though-wall crack was present. The observations are included in the figure captions in the Appendices.

In addition to physical inspection of the samples, a number of additional ring-compression tests were conducted with the new Instron (Model 5566). As-received samples (Zry-4, ZIRLO, M5 and E110) were compressed to determine elastic stiffness from the load-displacement data as compared to the predicted ring stiffness ($K = F/d = [E\ w\ t^3]/[1.8\ R^3]$, where E is Young's modulus, w is the width or length of the ring, t is the ring thickness, and R is the mean radius of the ring). For the as-received samples, measured K values for Zry-4 and ZIRLO were, on the average, 0.88 kN/mm compared to a predicted value of 0.86 kN/mm. Similarly, for the thicker as-received M5 samples the average (1.12 kN/mm) of the measured values was in good agreement with the predicted value (1.07 kN/mm). In addition, as-received and oxidized samples were compressed to a limited displacement. Test results for as-received samples limited to 2-mm cross-head displacement proved most interesting. For Zry-4 and ZIRLO, the offset method predicted 1.18 mm of permanent displacement, while direct post-test measurement gave 1.00 mm. For M5, the offset displacement was 0.13 mm higher than the direct post-test measurement. Because of these results, along with uncertainties regarding displacement due to partial cracking vs. plastic displacement, an offset displacement of 0.2 mm (2% nominal hoop strain) was taken as the transition strain between ductile and brittle behavior for these tests. This was then confirmed by compressing a highly oxidized sample through the first significant load drop; the offset displacement was 0.31 mm, while the post-test diameter decrease was 0.11 mm.

Tests on as-received and oxidized samples that were limited to 2 mm displacement were also interesting with regard to the evolution of deformation and failure. For very low-ductility samples, through-wall failure appears to occur first at the loading (0˚) and support (180˚) points, followed by failure at positions ±90˚ from the load application point. For intermediate-ductility samples, the loading and support locations tend to flatten out as the material deforms, followed by cracking of the brittle layers, and either through-wall failure or buckling followed by through-wall failure. Such behavior accounts for the wide variation in the rates of load decrease observed in the load-displacement curves for intermediate ECR samples. As the flattening and buckling of the load and support portions of the ring involve relatively high bending strains, the normalization of displacement to outer diameter is not an accurate metric for high-ductility rings.

Detailed analyses of the load-displacement curves in Appendices A and C, along with post-test physical examination of the samples and displacement-limited test results, were used to determine the offset displacement and plastic hoop strain prior to through-wall failure. These are listed in Table 4 for samples oxidized at 1000˚C and Table 5 for samples oxidized at 1100˚C. Graphical representation of these results is shown in Figs. 4 and 5, respectively. Figures 4a and 5a show ductility vs. measured ECR, while Figs. 4b and 5b show ductility vs. the CP-predicted ECR for M5 (0.61-mm wall) and Zry-4 (0.57-mm wall). Based on these data, essentially all of the samples tested exhibited offset strains >2% and were classified as "ductile". One sample (M5 oxidized at 1100˚C to 19.1% ECR with 1.8% offset strain) exhibited an offset strain slightly less than 2%. In such cases, the standard procedure adopted in this study is to repeat the test on a new sample with a slightly larger ECR. As shown in Table 5, a new M5 sample was oxidized to 20.6% ECR at 1100˚C. The test was interrupted after the first significant load drop (see) Fig. C.13 to allow direct measurement of diameters along, and perpendicular to, the loading direction. The offset strain was 3.2% as compared to the measured diameter decrease and increase values of 1.2% and 0.8%, respectively. Although more tests would be needed to better determine the ring-compression ductility of M5 at ≈20% measured ECR, the results for the second sample oxidized to 20.6% ECR at 1100˚C suggest that M5 retains ductility under these conditions.

In order to better quantify the sharp decrease in M5 ductility with increase in measured ECR (see Fig. 4a), an additional sample was oxidized at 1000˚C for 700-s longer than the 13.3% ECR M5 sample. Surprisingly, the measured weight gain decreased and the ECR decreased (13.3% at a CP-equivalent time of 3364 s to 12.4% at a CP-equivalent time of 4064 s). Both samples exhibited shiny black oxide layers with no evidence of spallation. The 12.4% ECR sample was sectioned to produce an 8-mm-long ring and subjected to ring compression testing with the displacement interrupted after the first significant load drop (see Fig. C.7). The offset strain was 2.5%, as compared to directly measured (post-test) diameter decrease and increase values of 2.1% and 1.2%, respectively. The results of this additional test confirm the low ductility of M5 at ≈13% measured ECR. However, the decrease in M5 ductility is much more gradual when plotted vs. CP-predicted ECR (see Fig. 4b), which varies with the square-root of time.

Figure 6 shows the post-test samples for Zry-4 oxidized at 1000˚C (a) and 1100˚C (b). Similarly, Fig. 7 shows the post-test samples for M5 oxidized at 1000˚C (a) and 1100˚C (b). The ECR values listed for identification are CP-calculated values, not measured values. See Tables 4 and 5 for the measured values. As some of these samples were handled and manually deformed to failure prior to photographing, refer to the figure captions in the Appendices for the actual condition of the samples following testing and prior to handling.

Table 4 Ring Compression Test Results for Samples Oxidized at 1000˚C and Quenched (see Table 2). Tests were performed on 8-mm-long samples at room temperature and at 2 mm/min. cross-head displacement rate. A complete set of tests were performed using the Model 4505 Instron. Some confirmation tests were performed with the new Model 5566 Instron on 8-mm-long rings cut from the same 25-mm-long oxidation samples.

Cathcart-Pawel ECR, %	Material	Measured ECR %	Offset Displacement mm	Offset Hoop Strain %	Confirmation Tests Model 5566 Instron
5	Zry-4	6.1	4.4	46	---
4.7	M5	4.3	4.6	48	--- ---
10	Zry-4	11.0	2.74	29	Yes
9.3	M5	7.6	4.85	51	Yes
15	Zry-4	16.9	0.711	7.5	Yes
14.1	M5	10.7	3.76	40	Yes
17	Zry-4	19.3	0.483	5.1	---
16.0	M5	11.6	≤1.82	≤19	---
20	Zry-4	22.4	0.307	3.2	---
18.8	M5	13.3	0.307	3.2	---
20.7	M5	12.4	0.238*	2.5*	---

*Additional sample oxidized and ring-compression tested in Model 5566 Instron to better assess ductility of M5 at ≈13% ECR.

Table 5 Ring Compression Test Results for Samples Oxidized at 1100˚C and Quenched (see Table 3). Tests were performed on 8-mm-long samples at room temperature and at 2 mm/min. cross-head displacement. A complete set of tests were performed using the Model 4505 Instron. Some confirmation tests were performed with the new Model 5566 Instron on 8-mm-long rings cut from the same 25-mm-long oxidation samples.

Cathcart-Pawel ECR, %	Material	Measured ECR %	Offset Displacement mm	Offset Hoop Strain %	Confirmation Tests Model 5566 Instron
5	Zry-4	6.2	5.5	58	---
4.7	M5	4.6	5.4	57	--- ---
10	Zry-4	10.9	1.9	20	---
9.3	M5	9.2	3.7	39	---
15	Zry-4	16.3	0.516	5.4	---
14.1	M5	13.8	0.709	7.5	Yes
17	Zry-4	18.0	0.38 - 0.56	4 - 6	---
16.0	M5	16.2	0.381	4.0	---
20	Zry-4	20.3	0.455	4.8	---
18.7	M5	19.1	0.170	1.8	---
20.2	M5	20.6	0.305*	3.2*	---

*Additional sample oxidized and ring-compression tested in Model 5566 Instron to better assess ductility of M5 at ≈20% ECR.

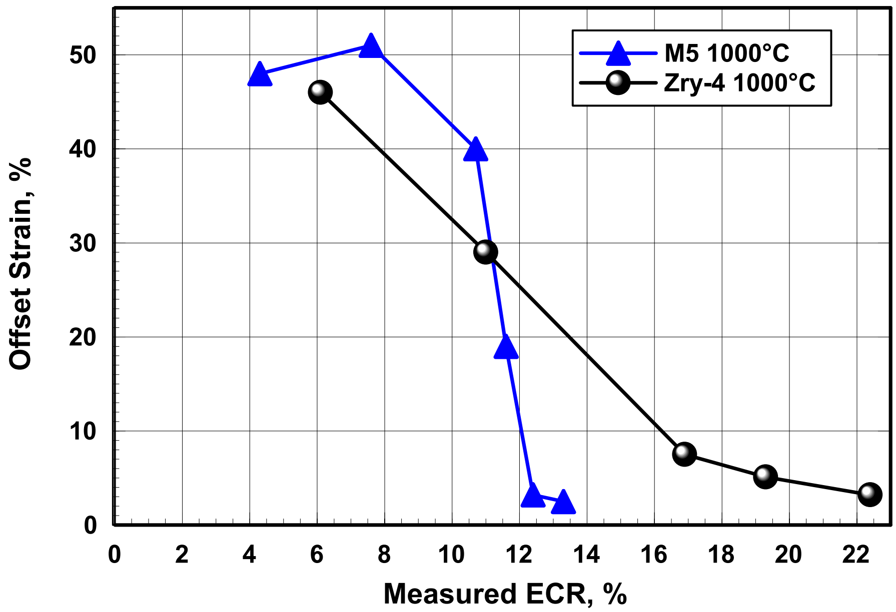

Fig. 4a. Post-quench ductility vs. measured ECR for M5 and Zry-4 oxidized in steam at 1000˚C. Ductility is based on offset strain determined from ring-compression tests conducted at room temperature and 2 mm/min. cross-head displacement rate.

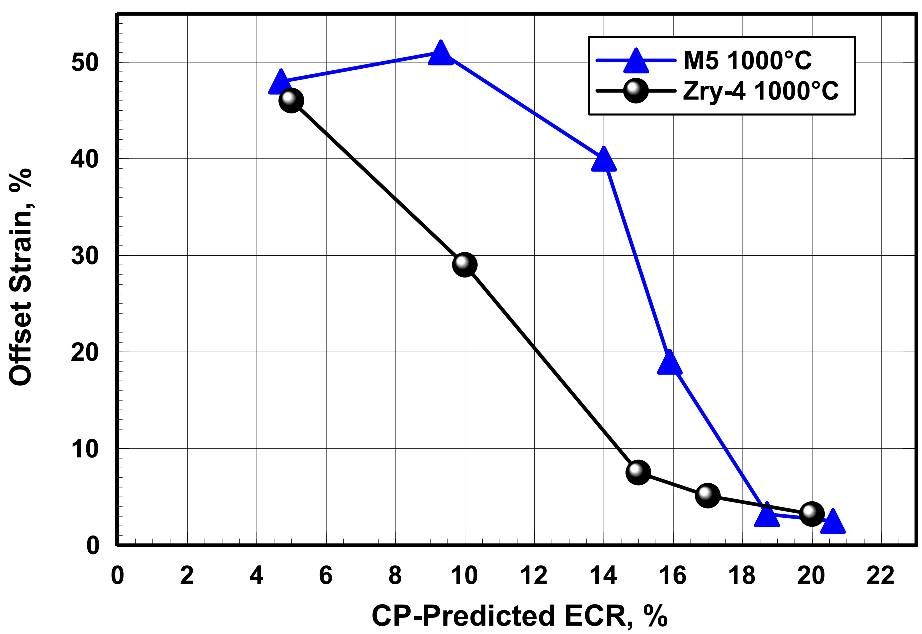

Fig. 4b. Post-quench ductility vs. CP-predicted ECR for M5 and Zry-4 oxidized in steam at 1000˚C. Ductility is based on offset strain determined from ring-compression tests conducted at room temperature and 2 mm/min. cross-head displacement rate.

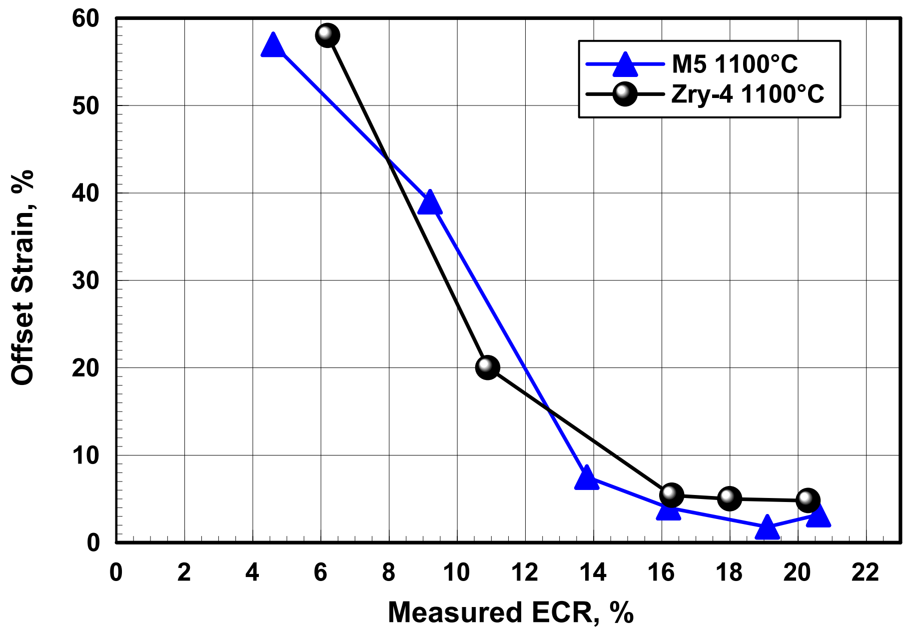

Fig. 5a. Post-quench ductility vs. measured ECR for M5 and Zry-4 oxidized in steam at 1100˚C. Ductility is based on offset strain determined from ring-compression tests conducted at room temperature and 2 mm/min. cross-head displacement rate.

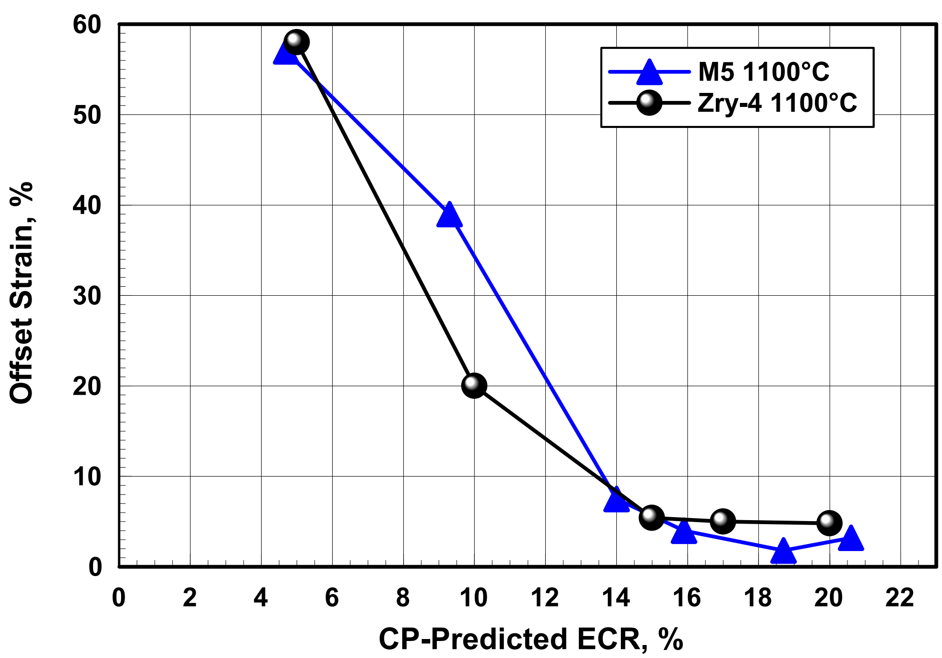

Fig. 5b. Post-quench ductility vs. CP-predicted ECR for M5 and Zry-4 oxidized in steam at 1100˚C. Ductility is based on offset strain determined from ring-compression tests conducted at room temperature and 2 mm/min. cross-head displacement rate.

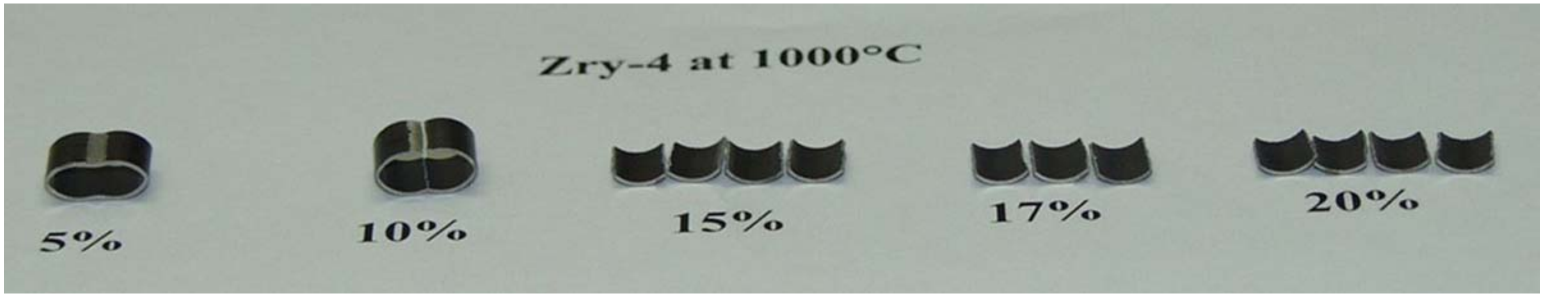

(a)

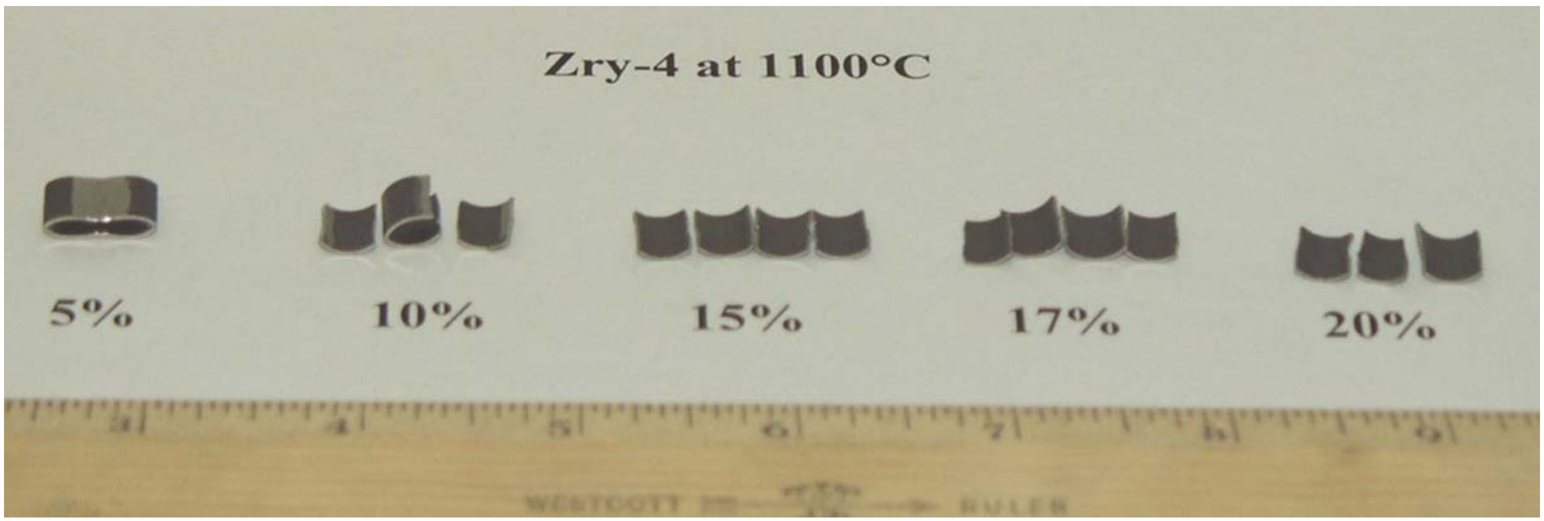

(b)

Fig. 6. Post-test appearance of Zry-4 ring-compression samples tested at room temperature and 2 mm/min: (a) samples oxidized at 1000˚C; and (b) samples oxidized at 1100˚C. ECR values are calculated using the Cathcart-Pawel weight gain correlation.

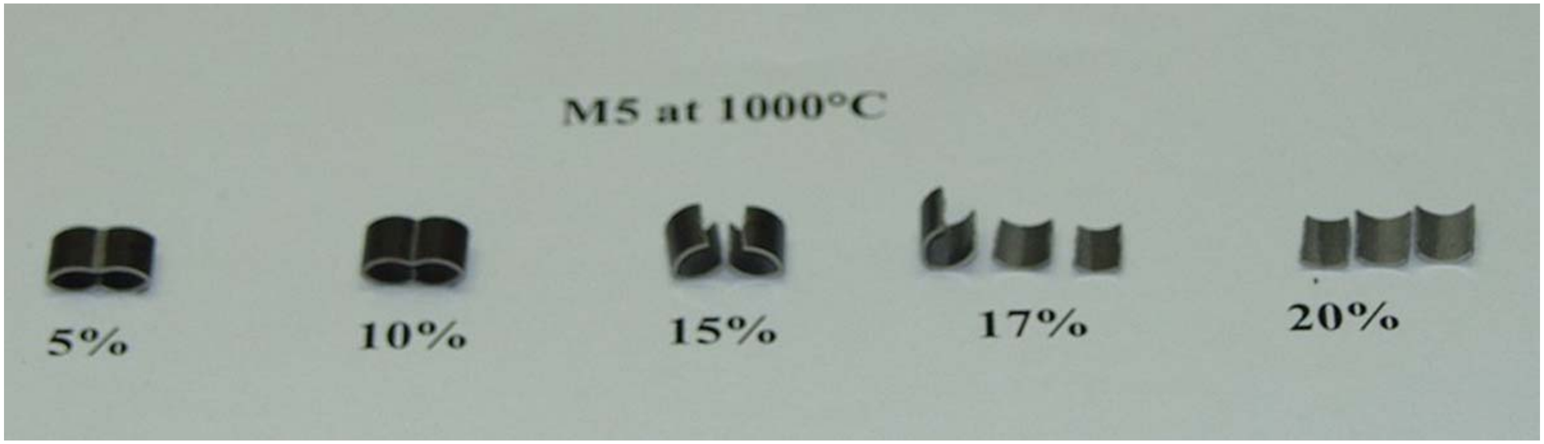

(a)

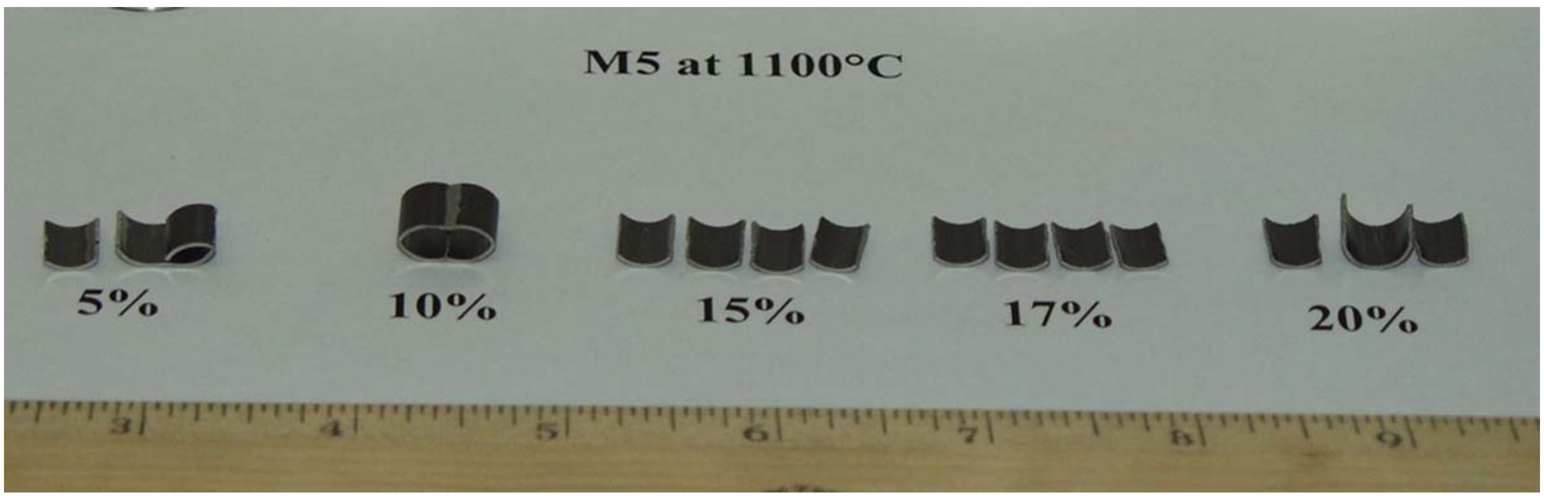

(b)

Fig. 7. Post-test appearance of M5 ring-compression samples tested at room temperature and 2 mm/min: (a) samples oxidized at 1000˚C; and (b) samples oxidized at 1100˚C. ECR values are calculated using the Cathcart-Pawel weight gain correlation and a wall thickness of 0.57 mm.

3.3 Post-test Characterization of Highest ECR Samples

Given that the ring compression test is really a structural test, as compared to a materials test, it is important to characterize the material to verify that it should behave in a ductile manner in the ring-compression test. From a materials perspective, it is essential that the hydrogen content be relatively low (<100 wppm) and that there be a sufficient amount of ductile, low-oxygen metal (prior-beta) remaining around the mid-radius of the sample. The hydrogen content was measured using the LECO Hydrogen Determinator.

Table 6 summarizes the results of the post-test characterization for Zry-4 and M5 samples at the highest ECR values. At 1000˚C, the hydrogen pickup for Zry-4 and M5 is low (≈20 wppm) indicating that protective oxide layers are still in place. Oxide layer thicknesses were measured from metallographic images for both alloys using a linear-intercept method and standard averaging techniques. From the arc segments in Fig. 8, it is clear that the oxide layer thicknesses follow the same trend as the weight gains: M5 < Zry-4. However, these oxide layer thicknesses do not scale directly with the weight gains: M5/Zry-4 oxide-layer-thickness ratio = 41%; M5/Zry-4 weight-gain ratio = 64%. There are two factors to consider in rationalizing these results: the thicker M5 may pick up more oxygen and the oxygen concentration in the M5 metal may be higher than for Zry-4 because the diffusion barriers are smaller (oxide layer) and/or less uniform (alpha layer). It is clear from the metallography, as well as the microhardness data, that the prior-beta layer consists of low-to-intermediate oxygen-containing metal for both M5 and Zry-4. However, is difficult to quantify the oxygen content in the various phases based on these results alone.

The results for the samples oxidized at 1100˚C for ≈1100 s indicate low hydrogen pickup and comparable oxide layer thicknesses (see Table 6 and Fig. 9). Unlike the results at 1000˚C, these oxide layer thicknesses are in proportion to the weight gain for the two alloys. Detailed evaluation of the metallographic and microhardness results is still in progress.

Table 6 Summary of Characterization of Highly Oxidized Zry-4 and M5 Samples after Exposure to Steam at 1000˚C and 1100˚C, Slow-cooling to 800˚C and Water Quench

Oxidation Temperature ˚C	Parameter	Zry-4	M5
1000	Effective Time, s	3364	3364
	Weight Gain, mg/cm^2	14.6	9.2
	Measured ECR, %	22.4	13.3
	Offset Displacement, mm	0.307	0.307
	Ductility, %	3.2	3.2
	H Content, wppm	19	26
	Hydrogen Pickup, wppm	15	22
	OD/ID Oxide Thickness, µm	83/82	36/32
	Microhardness within Middle 0.2 mm, DPH	290-420	300-430
1100	Effective Time, s	1065	1065
	Weight Gain, mg/cm^2	13.2	13.3
	Measured ECR, %	20.3	19.1
	Offset Displacement, mm	0.455	0.170
	Ductility, %	4.8	1.8
	H Content, wppm	22	17
	Hydrogen Pickup, wppm	19	12
	Oxide Layer Thickness, µm	70/68	72/62
	Microhardness within Middle 0.2 mm, DPH	240-470	260-400

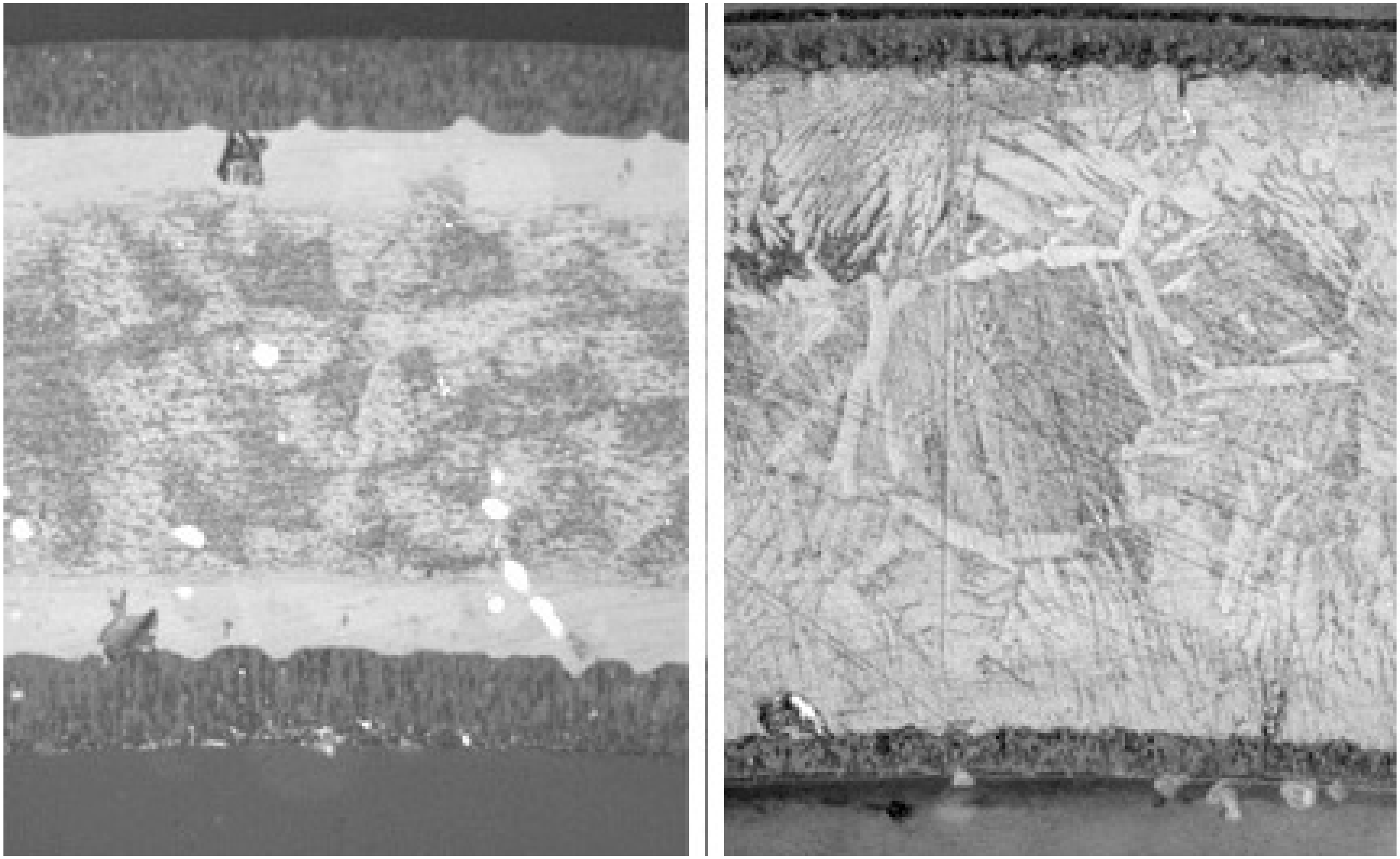

(a) Zry-4 (b) M5

Fig. 8. Metallography of as-polished Zry-4 (a) and M5 (b) oxidized in steam at 1000˚C for ≈3400 s, slow cooled to 800˚C and water quenched. Measured ECR values are 22.4% for Zry-4 and 13.3% for M5.

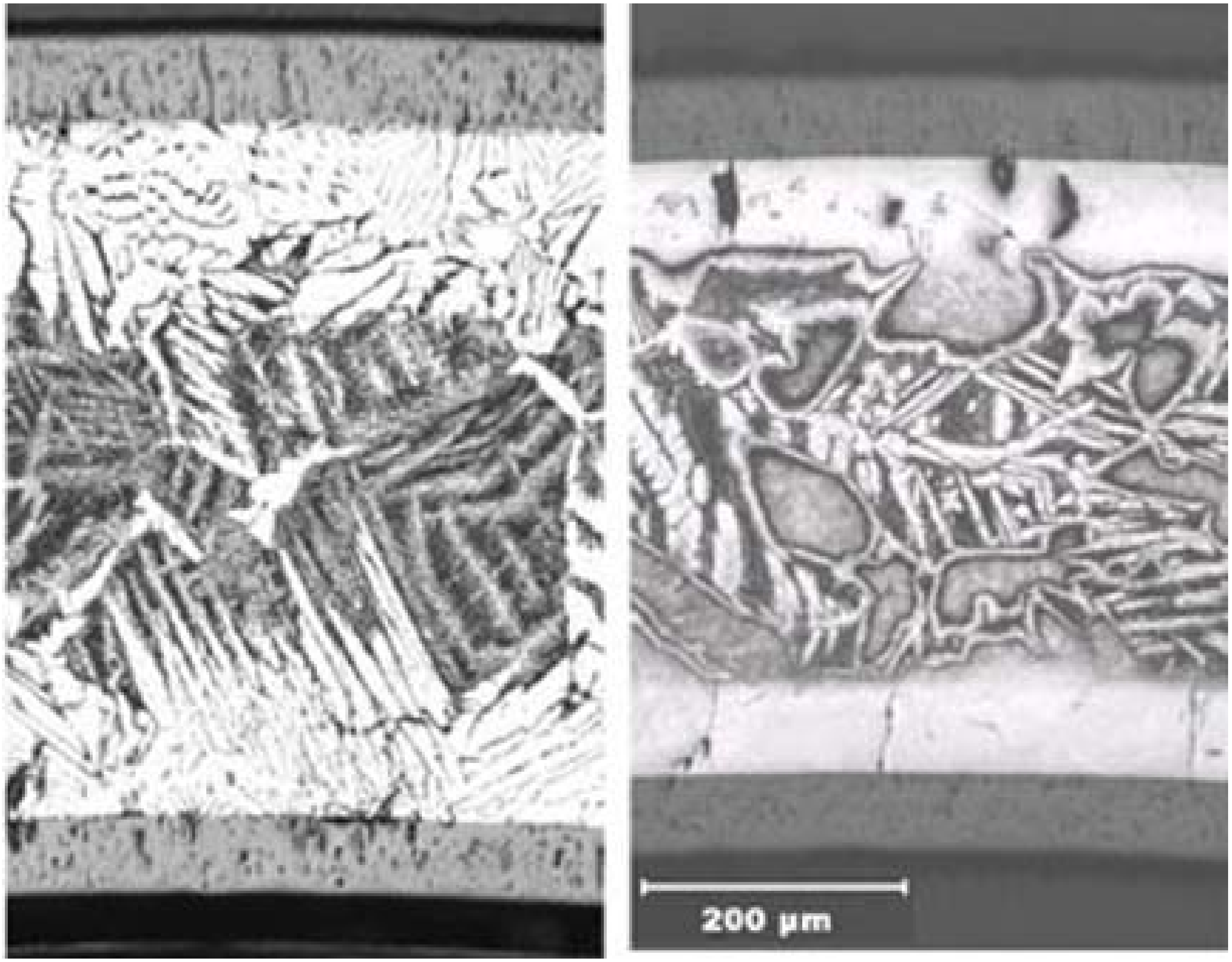

(a) M5 (b) Zry-4

Fig. 9. Metallography of etched M5 (a) and Zry-4 (b) oxidized in steam at 1100˚C for ≈1100 s, slow cooled to 800˚C and water quenched. Measured ECR values are 20.3% for Zry-4 and 19.1% for M5.

4. Summary of Results and Future Work

Weight gain measurements and ring-compression tests have been completed for Zry-4 and M5 cladding-alloy samples, which were oxidized in steam at 1000˚C and 1100˚C, slow-cooled to 800˚C and water quenched. 25-mm-long samples were exposed to two-sided oxidation for test times up to ≈3400 s at 1000˚C and up to ≈1100 s at 1100˚C. The individual test times were chosen to give Cathcart-Pawel (CP) calculated ECR values of 5, 10, 15, 17 and 20%. At 1100˚C oxidation temperature, all alloys exhibited about the same weight gain for each of the five test times and were in agreement with CP model predictions. At 1000˚C oxidation temperature, the weight gains for the alloys followed the expected trend with M5 < Zry-4. Maximum measured ECR values for the 1000˚C oxidations were 22.4% for the 0.57-mm-wall Zry-4 and 13.3% for the 0.61-mm-wall M5. Hydrogen pickup was low (<25 wppm) for all four high-ECR samples.

Ring-compression tests were performed at room temperature and a displacement rate of 2 mm/min. to determine post-quench ductility. The offset displacements determined from the load-displacement curves, normalized to the 9.50-mm outer diameter of the as-received cladding, were used as the measure of ductility. Samples with offset strains < 2% were classified as brittle. Based on this criterion, essentially all samples in the test matrix retained post-quench ductility. One sample (M5 oxidized for ≈1100 s at 1100˚C to 19% ECR) had an offset displacement of 1.8%. However, another M5 sample, oxidized to 21% ECR at 1100˚C, exhibited a post-quench offset strain of 3.2% and a directly measured strain of 1.2%. The average offset strain (2.5%) from these two tests suggests that M5 retains ductility at 1100˚C and ≈20% ECR. However, additional tests (≈3) would be required to obtain a better average value in this low-ductility regime.

Interpretation of the load-displacement curves proved to be very difficult for intermediate-ductility samples. One-to-two minor load drops did not necessarily indicate through-wall failure. Physical examination of the sample and additional displacement-limited tests were needed for these cases. For future testing, it is recommended that two ring compression samples be prepared for each oxidized sample. The ring prepared from 4-to-12 mm from the middle of the sample should be tested to maximum displacement to determine the overall shape of the load displacement curve. If this sample has at least one through-wall crack, the second ring cut from ±4 mm from the center should be tested with the displacement limited to the first significant load drop (sharp and large for high-ECR samples and more gradual for some intermediate-ECR samples). For displacement-limited tests, physical examination of the compressed ring can reveal the location and mode of the first through-wall failure, while direct post-test diameter measurements can be performed to support the ductility determined from the offset method.

In addition to hydrogen analysis, post-test characterization consisted of physical examination of all compressed samples, metallographic analysis of the oxidized-and-quenched samples at their highest ECR values, and radial profiling of microhardness for these high-ECR samples. Detailed evaluation of the metallographic and microhardness results is in progress to try to correlate the material structure – the amount of low-oxygen content metal remaining after oxidation – with the ring-compression results. Preliminary results are presented in the following. For Zry-4 oxidized at 1100˚C to 20% ECR, Fig. 10 shows well defined oxide and oxygen-stabilized (white) alpha layers. The inner and outer oxide and alpha layers are brittle at room temperature as indicated by Vickers hardness measurements >1000 DPH (diamond-pyramid hardness). The alpha incursions, slightly grayer than the alpha layers that formed at 1100˚C, have a Vickers hardness of ≈500 DPH, indicating that they probably formed at lower oxygen content during cooling from 1100˚C to 800˚C prior to quench. The gray-white and dark gray regions, within what was the beta layer at 1100˚C, contain intermediate-to-low oxygen content regions. The microhardness of the dark gray region is ≈300 DPH. This microhardness is consistent with values reported by Hobson and Rittenhouse [5] and Hobson [6] for the prior-beta layer after oxidation at 1066-1093˚C and rapid cooling. The low-hardness region in Fig. 10 is extensive enough to support the ductile behavior determined from the ring-compression tests.

Ring-compression results for samples oxidized at 1000˚C for ≈3400 s, prior to quench, are very interesting in that post-quench ductility values for both alloys are ≈3% even though the weight gains are very different. Figure 8 shows that the difference in oxide-layer thickness is in qualitative agreement with the difference in weight gain. But from Table 6, it can be seen that the M5-to-Zry-4 ratio of total oxide thickness is 41%, while the weight-gain ratio is 64%. This suggests that the oxygen pickup in the thicker M5 metal is higher than for Zry-4. To better understand whether these materials should behave in a ductile manner, it is important to examine their microstructures and microhardness. In Fig. 11, the etched microstructure of M5 is shown after oxidation for ≈3400 s at 1000˚C. This figure shows that the oxygen-stabilized alpha layers are not as uniform or well defined as they are for Zry-4 and that the prior-beta layer is a more complex mixture of phases, most likely with varying levels of oxygen. As listed in Table 6, microhardness values as low as ≈300 DPH were found near the middle of the M5 sample. However, it is difficult to quantify the extent of the low-oxygen-content ductile material for this alloy, especially as the phase diagram is not yet well characterized. More work is in progress to correlate microstructure with post-quench ductility.

In summary, the ring-compression test appears to be a reasonable screening test for post-quench ductility, especially for comparing the performance of alloys oxidized and tested under the same conditions. However, the "ductility" determined in this study, does not represent a material property as well defined as tensile-test uniform elongation. The ring-compression hoop bending stresses and strains, as well as the alpha incursions that lead to ductility decrease, are not uniform in the circumferential direction. Different quantitative results would have been obtained with changes in oxidation (one-sided vs. two-sided), changes in sample cooling rate (quench from oxidation temperature vs. quench from 800˚C), changes in load-support design (curved vs. flat), and changes in ring-compression test conditions (strain rate and temperature). Also, the demonstration of ductility in non-deformed rings with very little hydrogen pick-up does not guarantee that ballooned-and-burst cladding with corrosion-induced hydrogen pickup and/or with secondary hydriding from inner-surface oxidation would behave in a ductile manner.

Future work consists of completing the test matrix for the 1200˚C and 1260˚C oxidation temperatures and completing the correlation between ring-compression ductility and microstructure/chemistry of the alloys. The 1200˚C Zry-4 samples have been prepared. Work is in progress to prepare M5 samples at 1200˚C and both alloys at 1260˚C. M5 and Zry-4 LOCA integral tests will be performed at 1000˚C, 1100˚C and 1200˚C and 17% ECR (calculated). Such tests would generate samples with a ballooned-and-burst region and with secondary hydriding in the neck and beyond-neck regions. The ANL-proposed method of determining post-quench ductility is to subject the LOCA post-quench samples to a four-point-bend-test, followed by ring compression tests for 8-mm-long rings cut from the beyond-neck region.

Fig. 10. Microstructure of etched Zry-4 after oxidation at 1100˚C for ≈1100 s, slow cooling to 800˚C and quench. Microhardness values of the oxide and oxygen-stabilized alpha layers are >1000 DPH, while microhardness of the alpha incursions is ≈500 DPH and microhardness of the low-oxygen, prior-beta layer is ≈300 DPH.

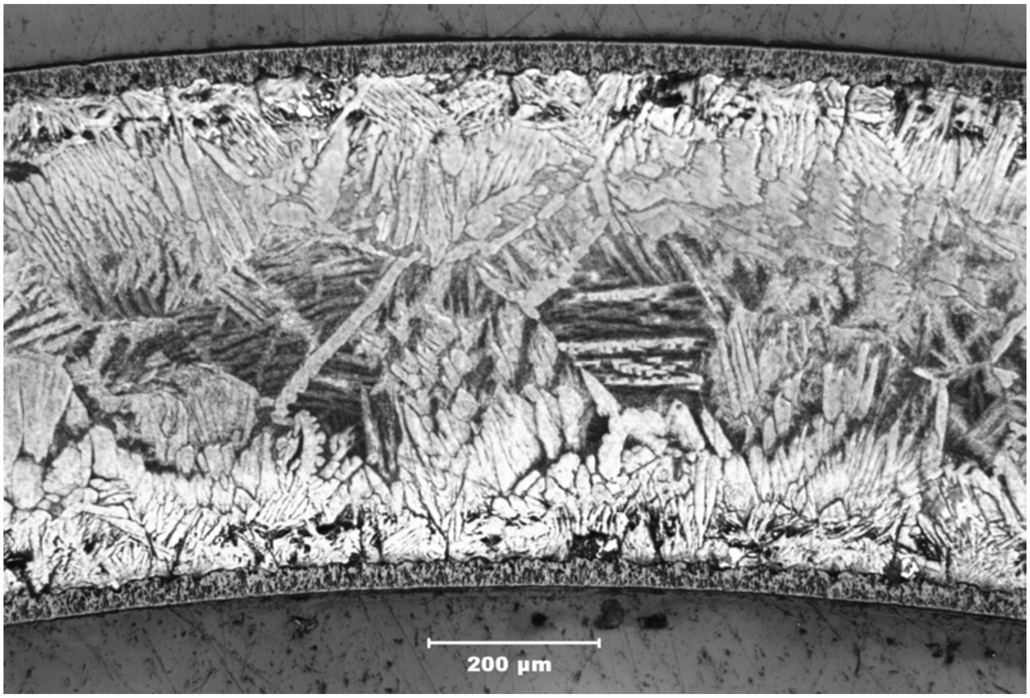

Fig. 11. Microstructure of etched M5 after oxidation at 1000˚C for ≈3400 s, slow cooling to 800˚C and quench.

References

1. Y. Yan, T. Burtseva and M. C. Billone, "Validation Test Results for M5 Post-Quench-Ductility Sample Preparation," letter report to NRC and Framatome, April 8, 2003.

2. Y. Yan, T. Burtseva and M. C. Billone, "Progress Report on Sample Preparation for Post-Quench-Ductility Tests of Westinghouse Zircaloy-4 and ZIRLO," letter report to NRC and Westinghouse, April 11, 2003.

3. Y. Yan, T. Burtseva and M. C. Billone, "Progress Report on E110 Post-Quench Ductility Test Program," letter report to NRC and RRC KI, May 31, 2003.

4. M. C. Billone, T. Burtseva and Y. Yan, "Hydrogen Pickup and Ring-Compression Ductility for E110 Oxidized in Steam at 1000˚C," letter report to NRC and RRC KI, January 31, 2004.

5. D. O. Hobson and P. L. Rittenhouse, "Embrittlement of Zircaloy-Clad Fuel Rods by Steam during LOCA Transients," ORNL 4758, January 1972.

6. D. O. Hobson, "Ductile-Brittle Behavior of Zircaloy Fuel Cladding," Proc. ANS Topical Mtg. on Water Reactor Safety, Salt Lake City, March 26, 1973, pp. 274-288.

APPENDIX A

Load-Displacement Curves for Oxidized-and-Quenched Zry-4 Samples Subjected to Ring-Compression Tests at Room Temperature and a Cross-head Displacement Rate of 2 mm/minute

Note: ECR values listed on the figures are approximate values. For more precise values, refer to Tables 4 and 5 in the main body of the report.

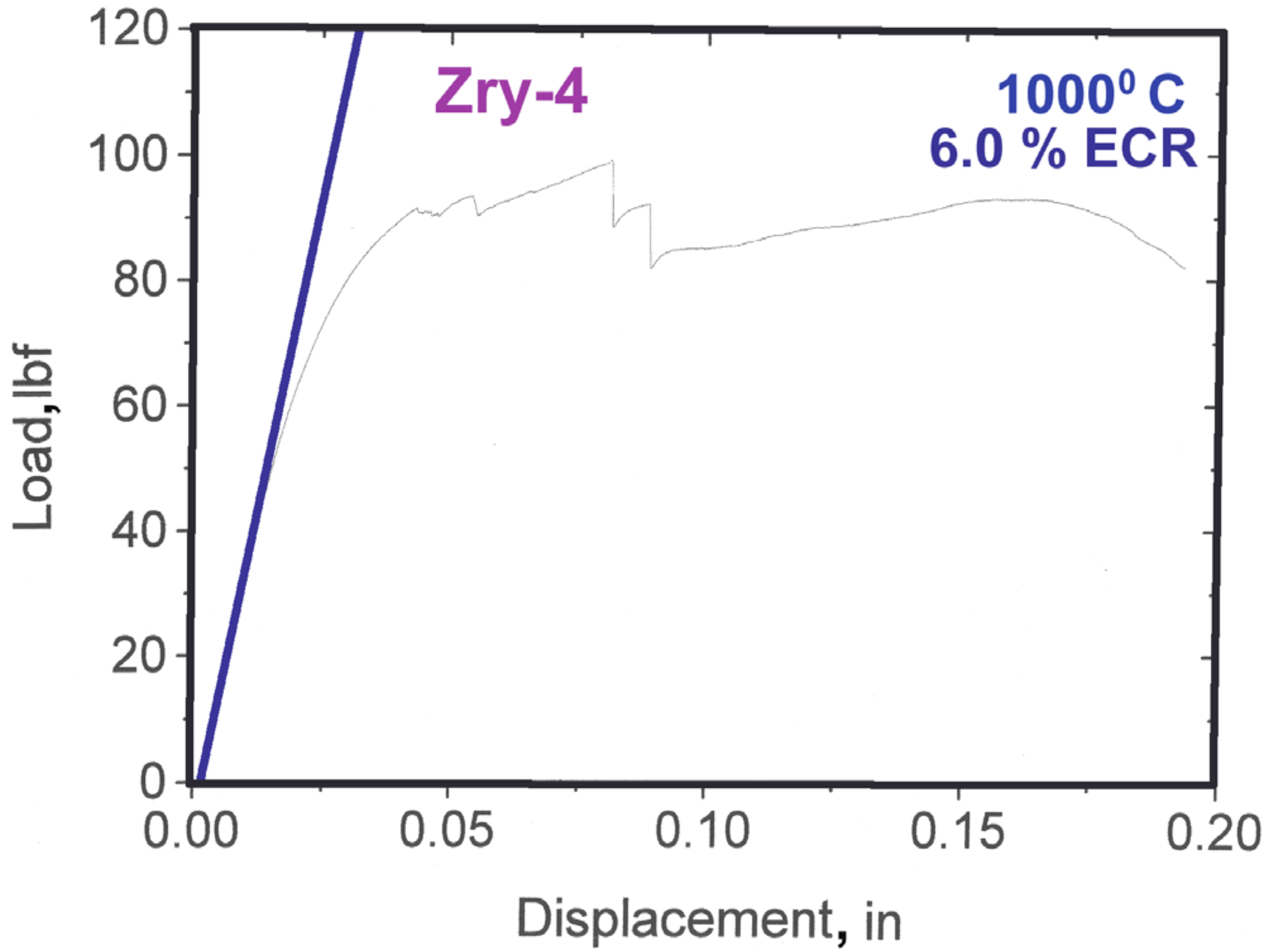

Fig. A.1 Ring-compression load-displacement data for Zry-4 oxidized to ≈6% ECR at 1000˚C. Sample was intact; no through-wall crack observed. Significant buckling observed. Oxide/alpha cracking, which should correspond to the two load drops, observed on buckled outside surface. Offset displacement of 4.4 mm was determined form the end point of the curve.

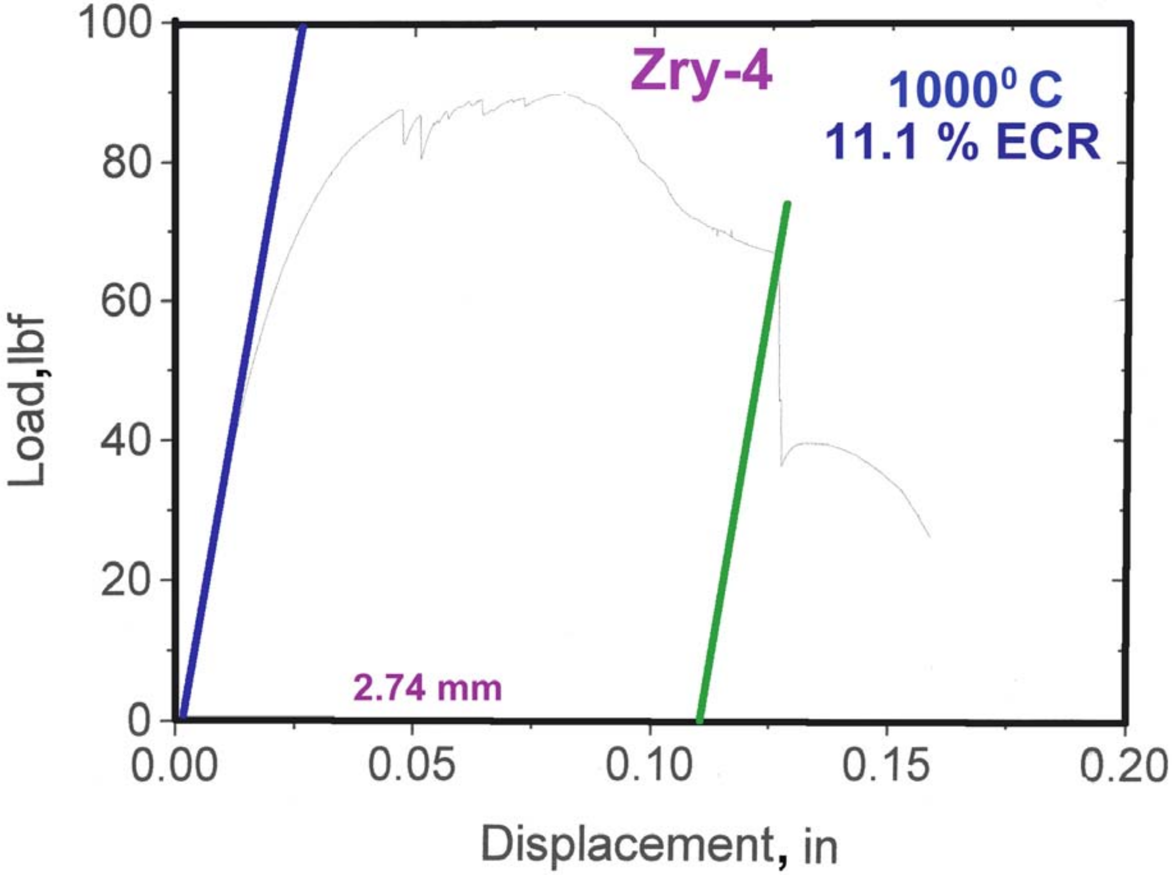

Fig. A.2 Ring-compression load-displacement data for Zry-4 oxidized to ≈11% ECR at 1000˚C. One through-wall crack, corresponding to large abrupt load drop, observed in buckled region. Local ductility in this buckled region is much higher than the 29% calculated from the 2.74 mm offset displacement.

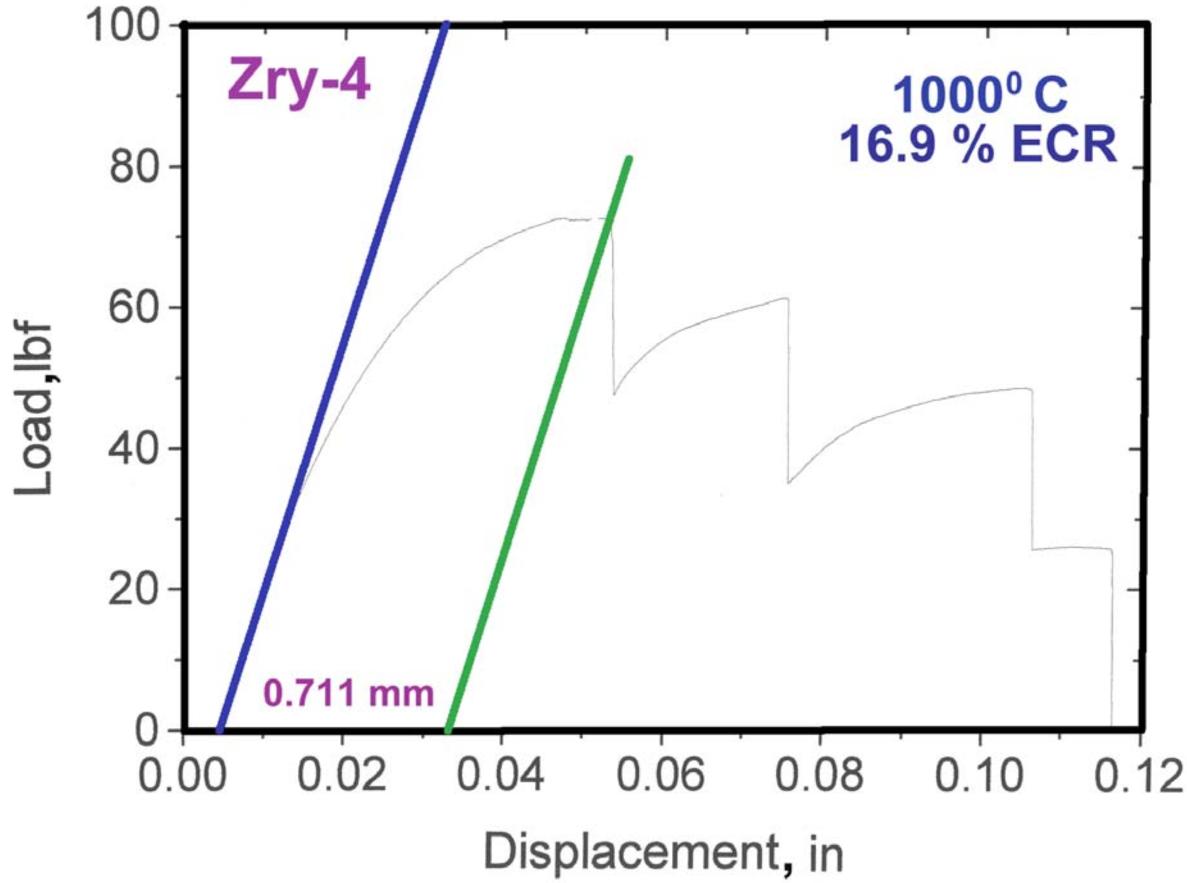

Fig. A.3 Ring-compression load-displacement data for Zry-4 oxidized to ≈17% ECR at 1000˚C. Four through-wall cracks observed.

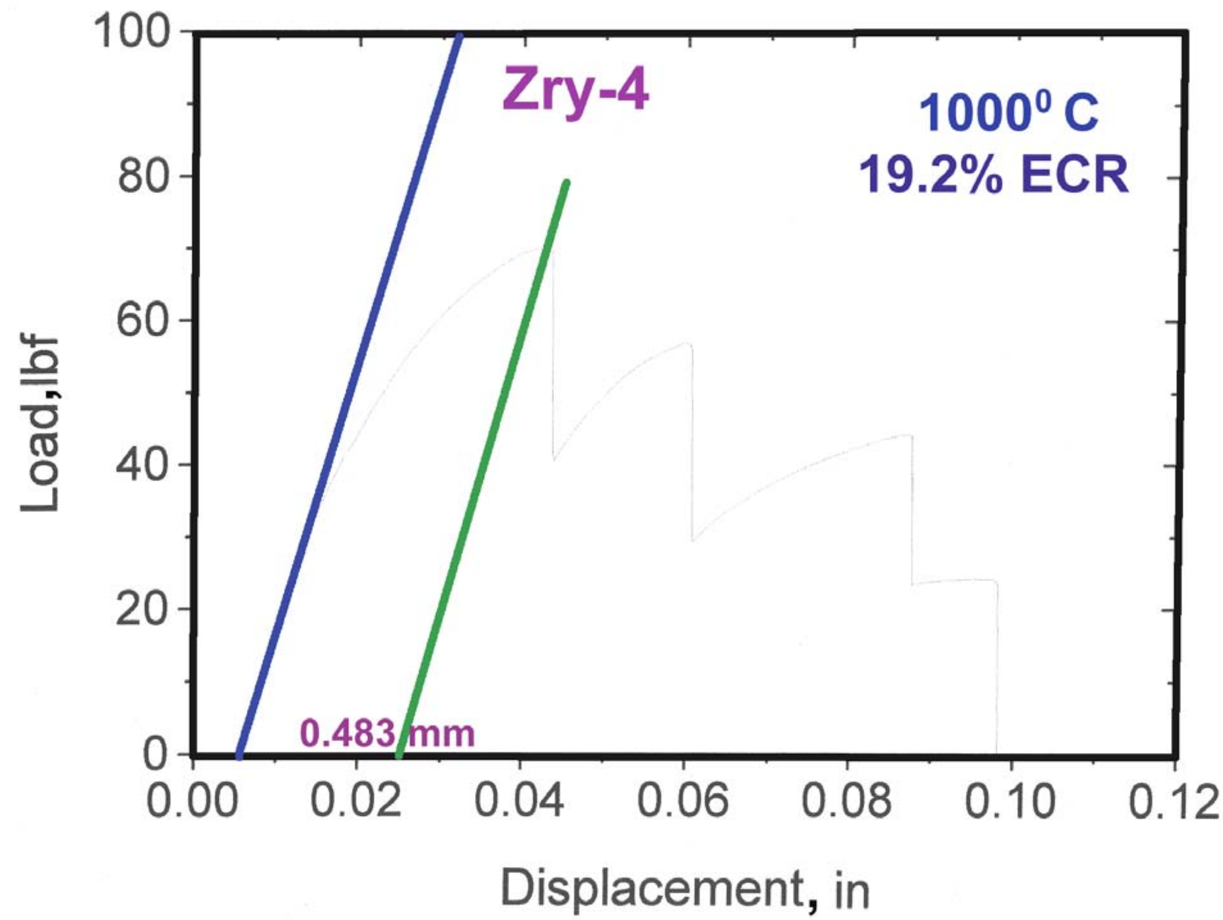

Fig. A.4 Ring-compression load-displacement data for Zry-4 oxidized to ≈19% ECR at 1000˚C. Four through-wall cracks observed.

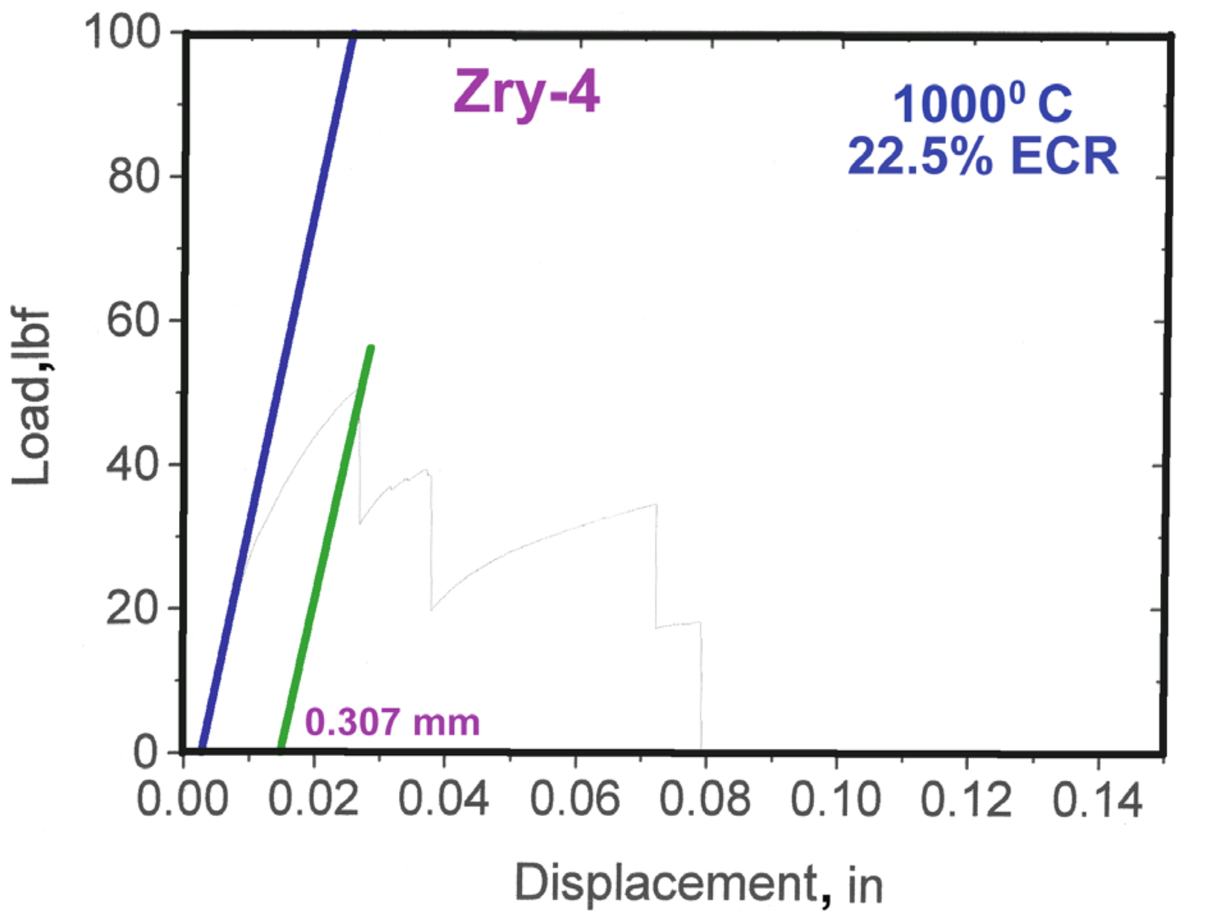

Fig. A.5 Ring-compression load-displacement data for Zry-4 oxidized to ≈22% ECR at 1000˚C. Four through-wall cracks observed.

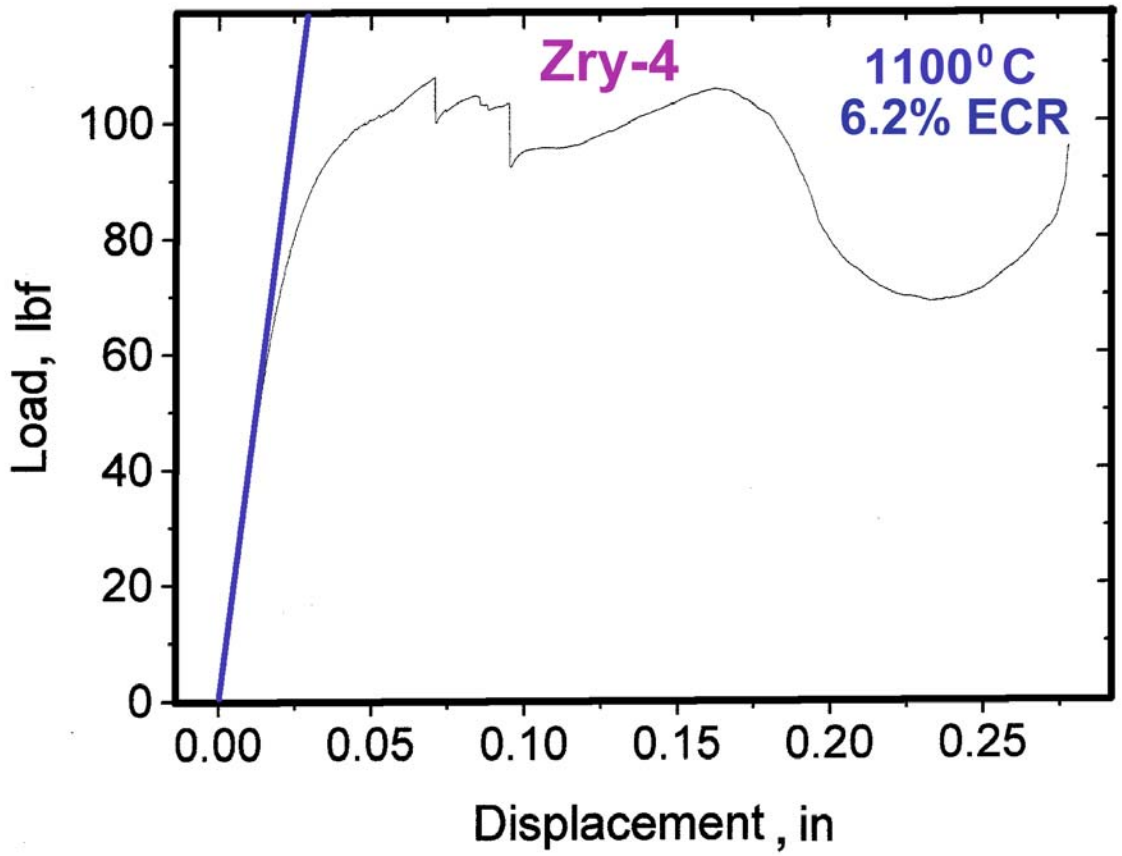

Fig. A.6 Ring-compression load-displacement data for Zry-4 oxidized to ≈6% ECR at 1100˚C. Sample intact; no through-wall crack. Significant buckling observed. Oxide/alpha cracking, which should correspond to the two load drops, observed on buckled outside surface. Offset displacement of 5.5 mm was determined by "unloading" from the point at 0.225" on the displacement axis prior to the upswing in load.

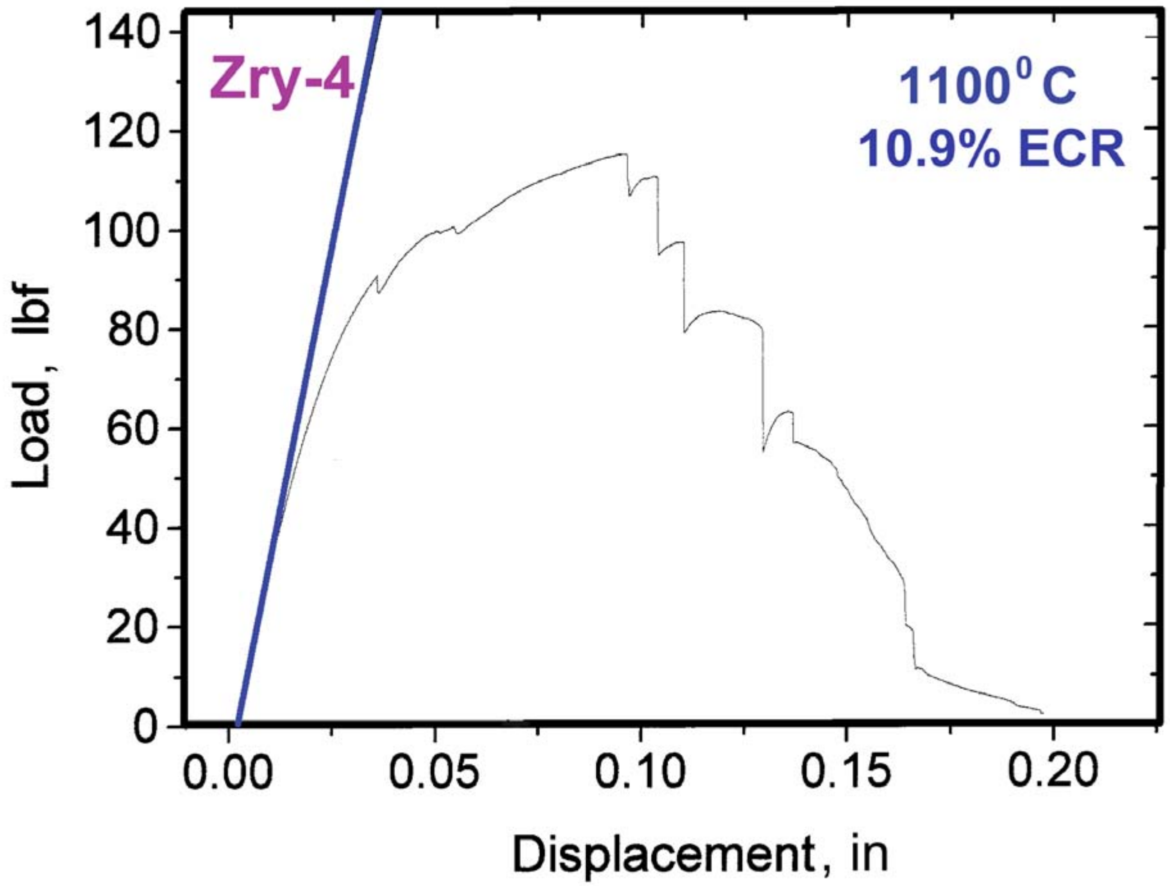

Fig. A.7 Ring-compression load-displacement data for Zry-4 oxidized to ≈11% ECR at 1100˚C. Three through-wall cracks and one partial-wall crack were observed. The first through-wall crack is associated with the second load drop, which corresponds to an offset displacement of 1.9 mm.

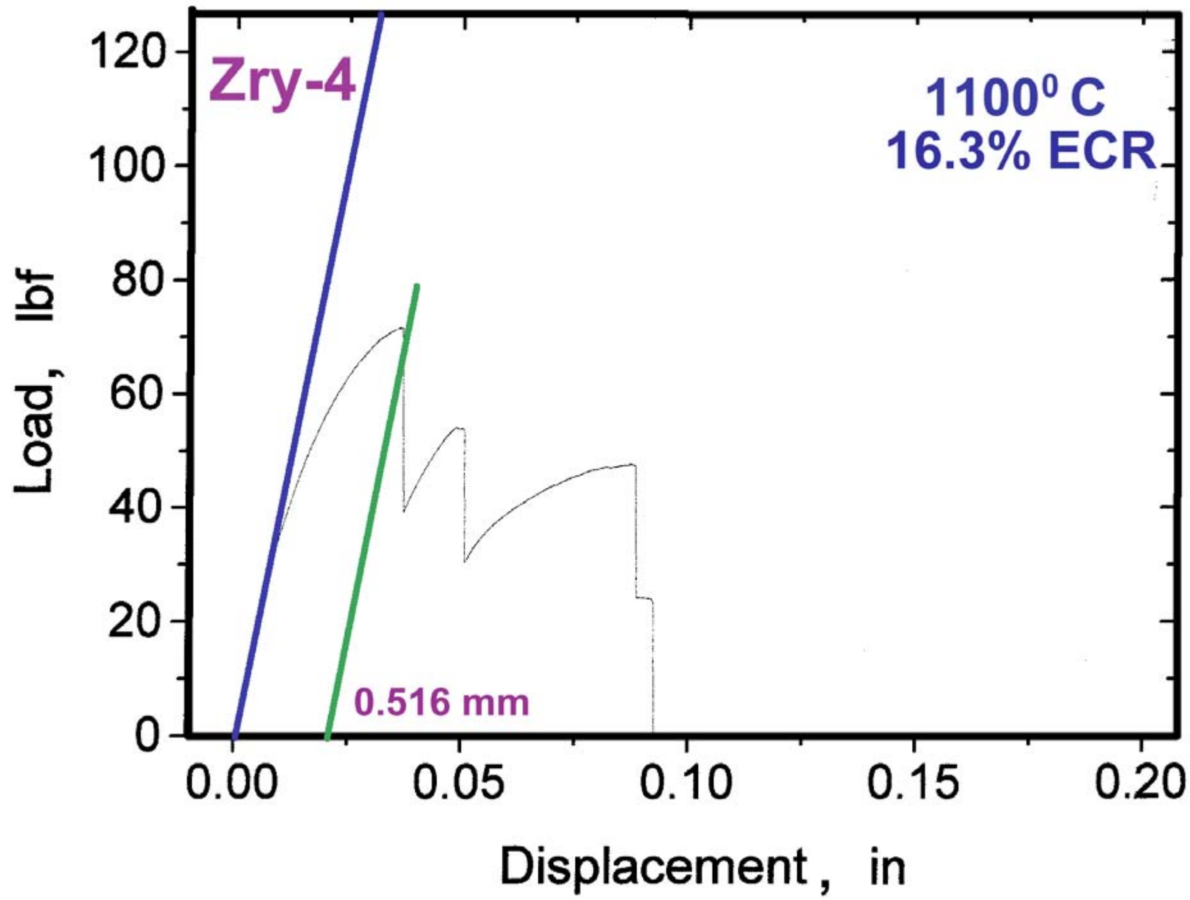

Fig. A.8 Ring-compression load-displacement data for Zry-4 oxidized to ≈16% ECR at 1100˚C. Sample fractured into four pieces with no evidence of buckling.

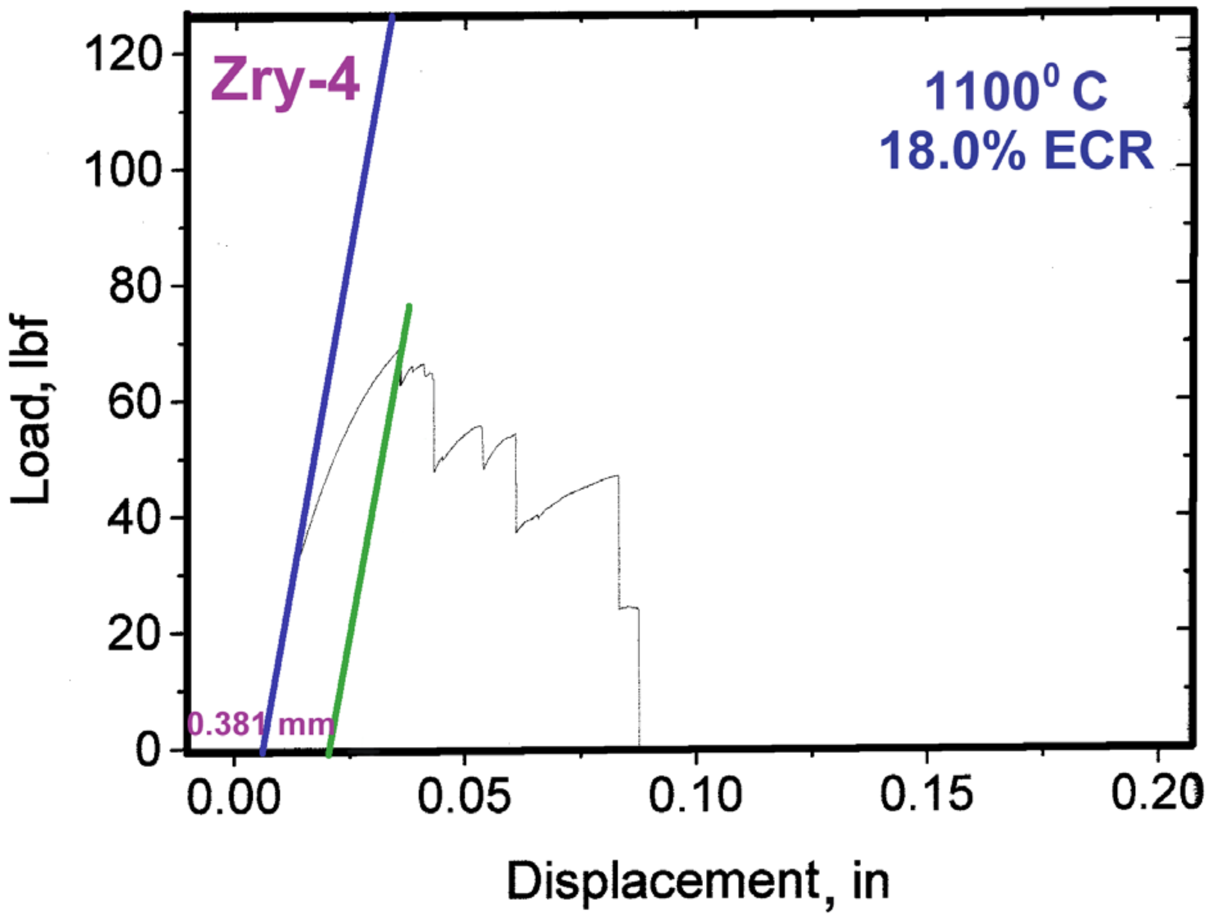

Fig. A.9 Ring-compression load-displacement data for Zry-4 oxidized to ≈18% ECR at 1100˚C. Sample fractured into 3 pieces. First through-wall crack likely developed at second load-drop, with an offset displacement of 0.56 mm. However, some of the apparent offset between 0.38 and 0.56 mm is due to crack displacement, rather than plastic deformation.

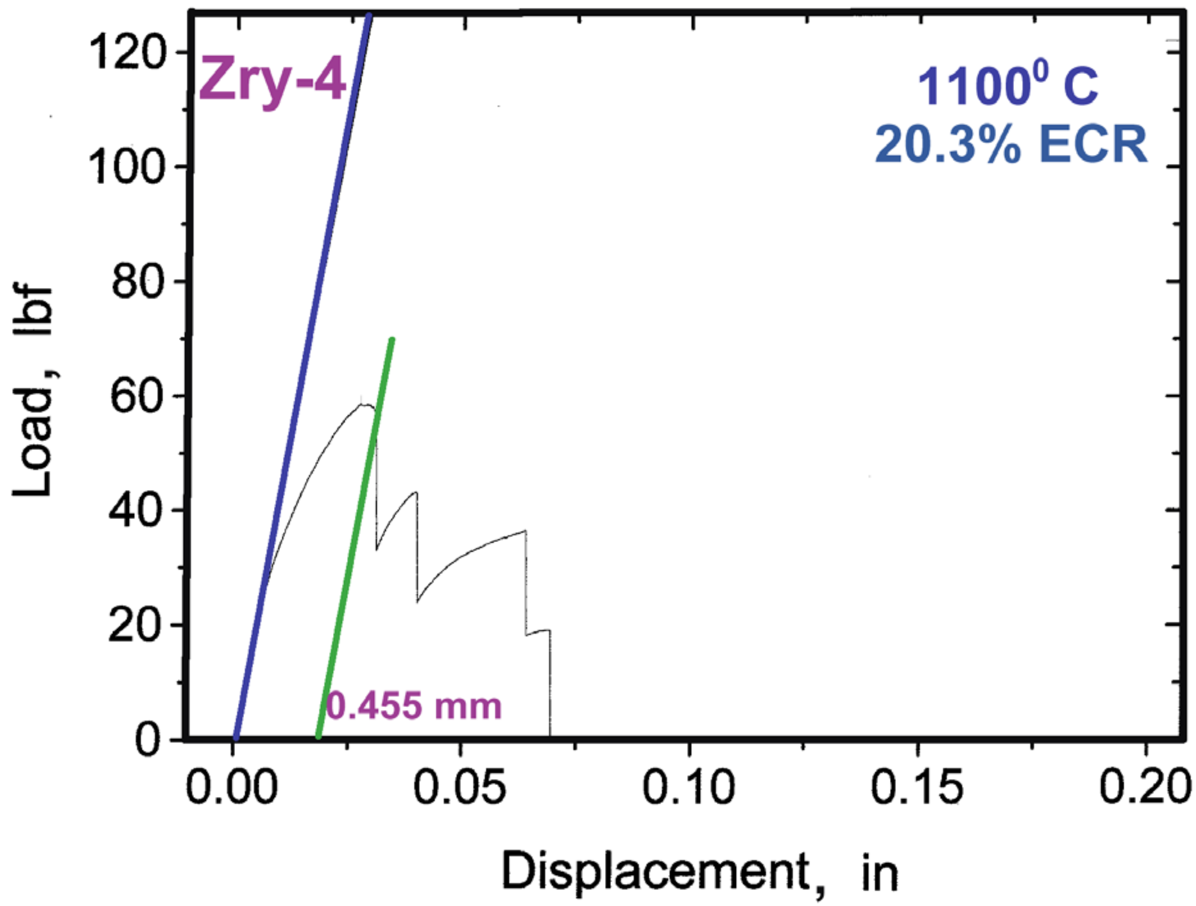

Fig. A.10 Ring-compression load-displacement data for Zry-4 oxidized to ≈20% ECR at 1100˚C. Sample fractured into four pieces, corresponding to the four load drops.

APPENDIX C

Load-Displacement Curves for Oxidized-and-Quenched M5 Samples Subjected to Ring-Compression Tests at Room Temperature and a Cross-head Displacement Rate of 2 mm/minute

Note: ECR values listed on the figures are approximate values. For more precise values, refer to Tables 4 and 5 in the main body of the report.

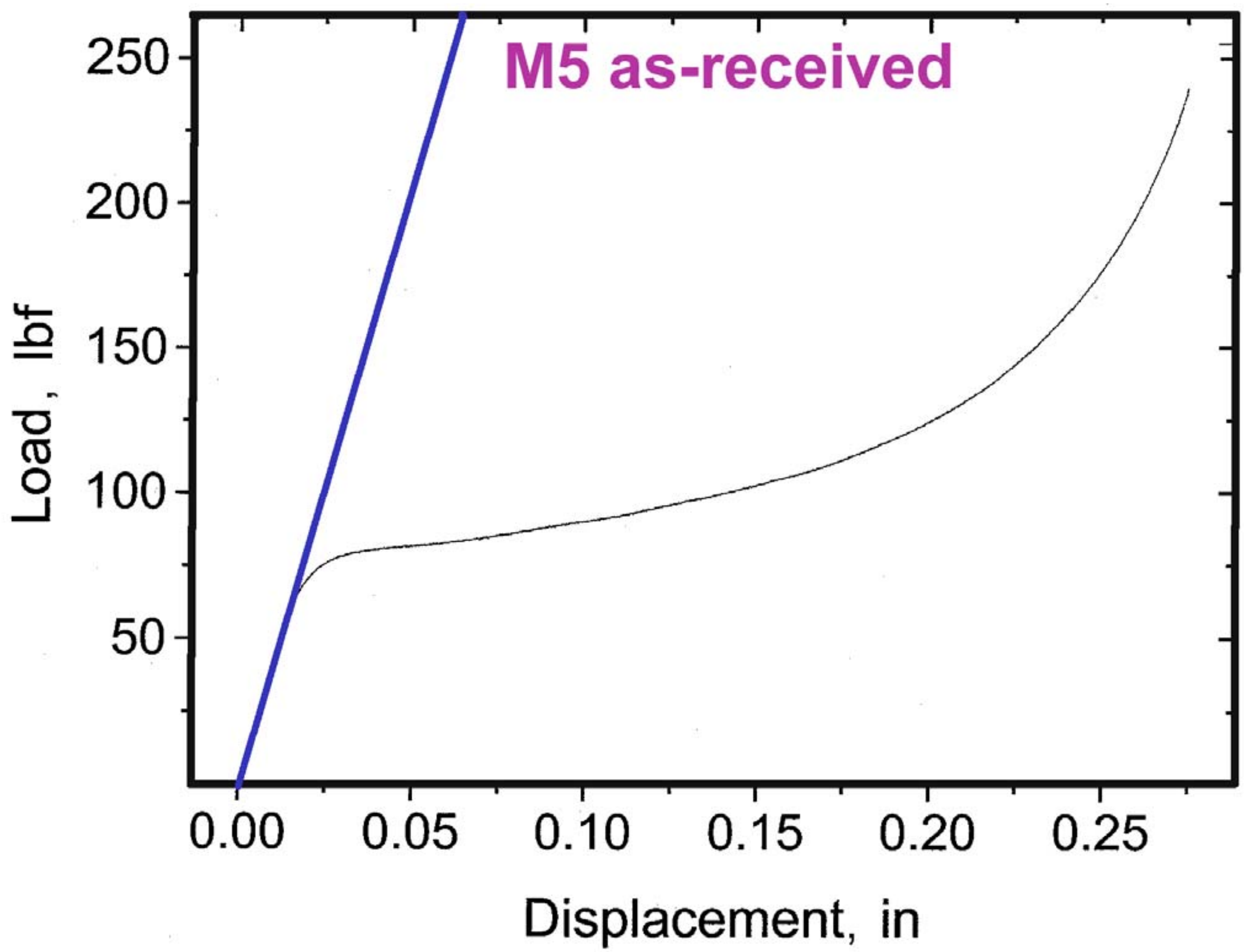

Fig. C.1 Ring-compression load-displacement data for as-received M5 (9.50-mm OD, 0.61-mm wall, 8-mm length). Specimen compressed "flat" with no through-wall crack. Mild buckling such that load center and support center locations are in contact.

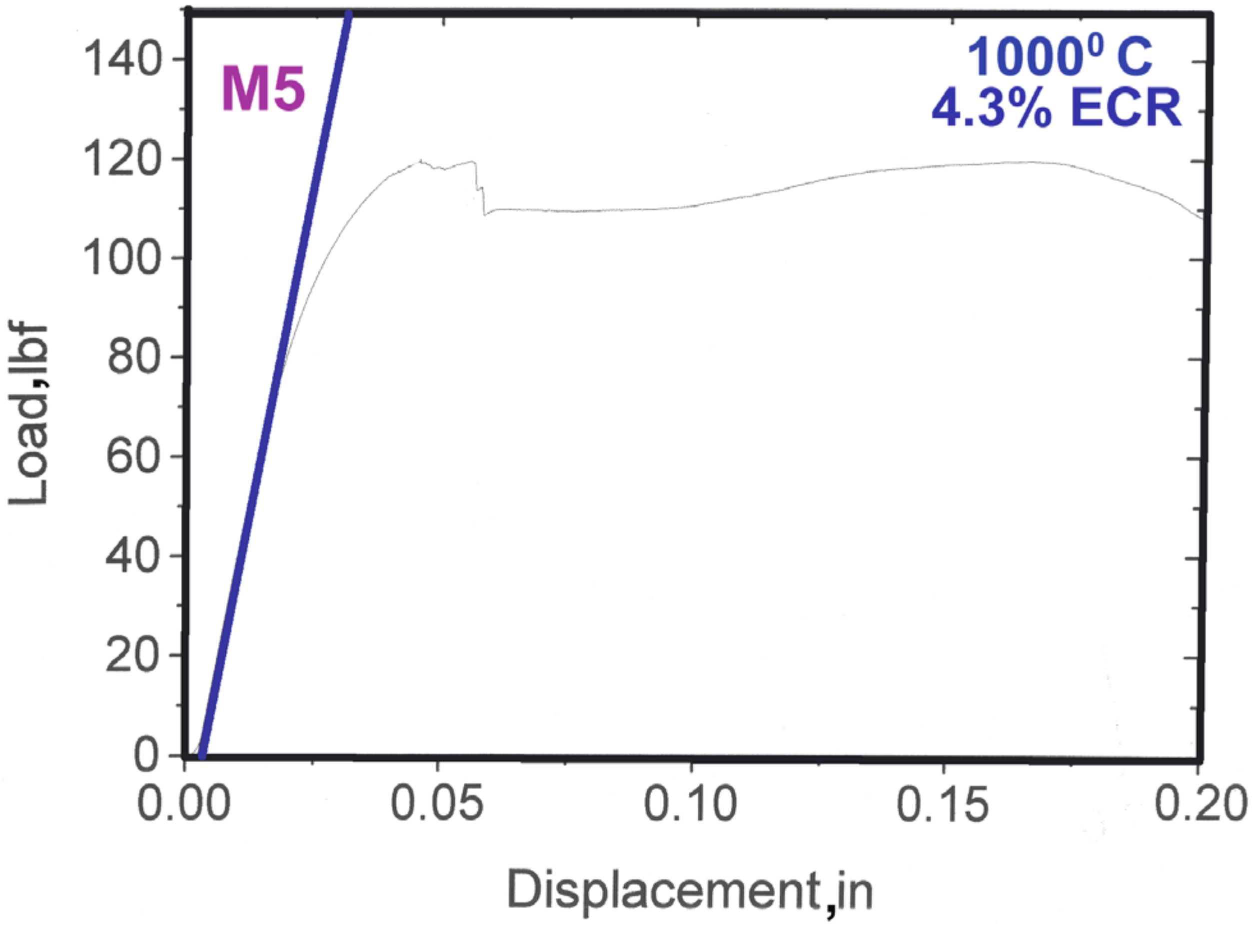

Fig. C.2 Ring-compression load-displacement data for M5 oxidized to ≈4% ECR at 1000˚C. Specimen compressed to within 2 mm of ID contact at 0˚ (load application) and 180˚ (support) locations. No through-wall crack observed. OD oxide/alpha cracking observed at 0˚, 90˚, 180˚ and 270˚; ID oxide/alpha cracking obseved at 90˚ and 270˚. Cracking and buckling appear to initiate at 1.3 mm total displacement. Offset displacement is determined to be 4.6 mm based on the end point of the curve.

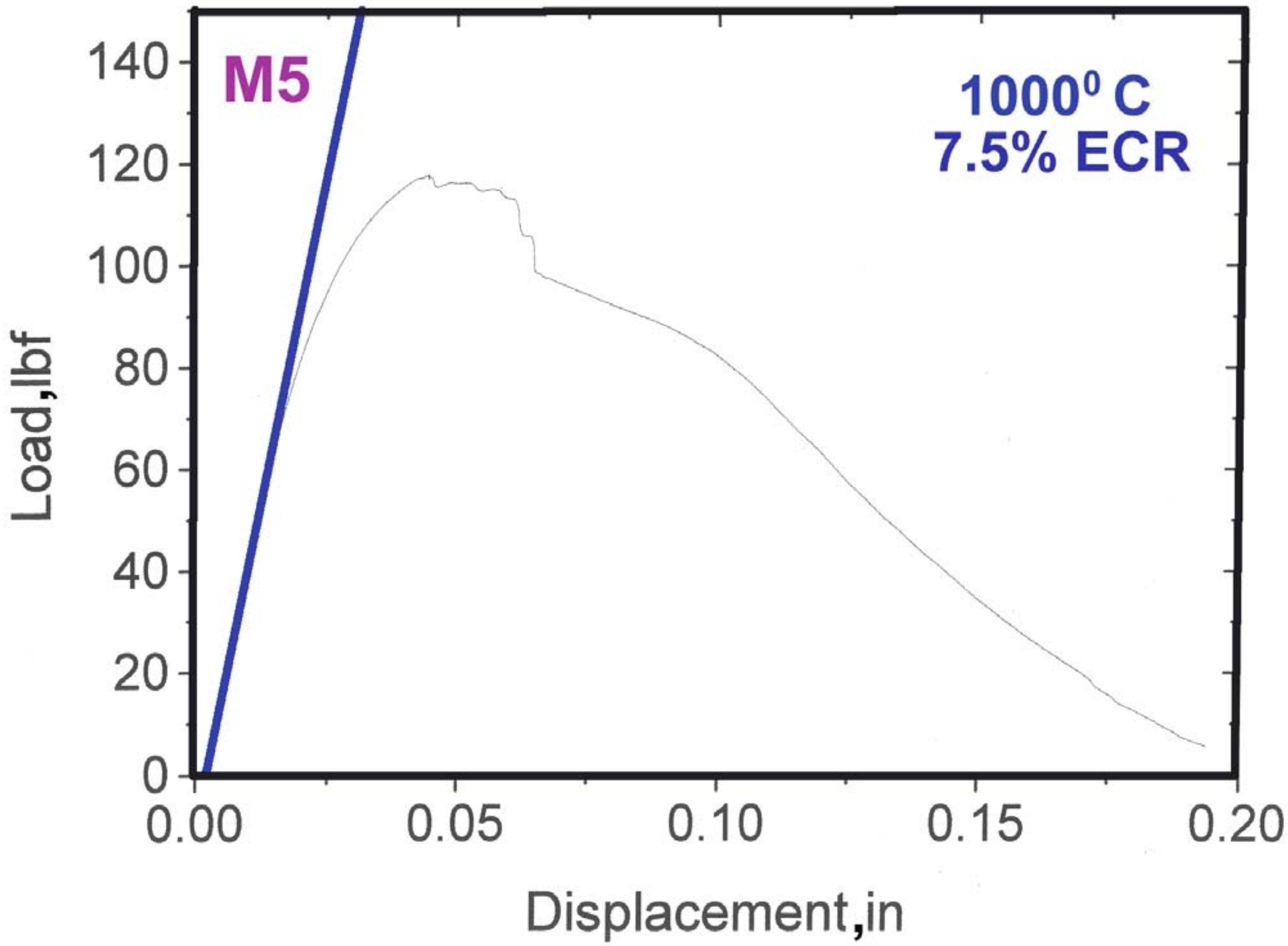

Fig. C.3 Ring-compression load-displacement data for M5 oxidized to ≈8% ECR at 1000˚C. Specimen compressed to within 2.5 mm of ID contact at 0˚ and 180˚ locations. No through-wall crack along whole length. ID and OD oxide/alpha cracking at all four locations appears to be complete at 1.1-mm off-set displacement. Gradual load decrease appears to be due to effects of buckling of the prior-beta region at 0˚ and 180˚. Offset displacement of 4.85 mm is based on unloading from the end point of the curve.

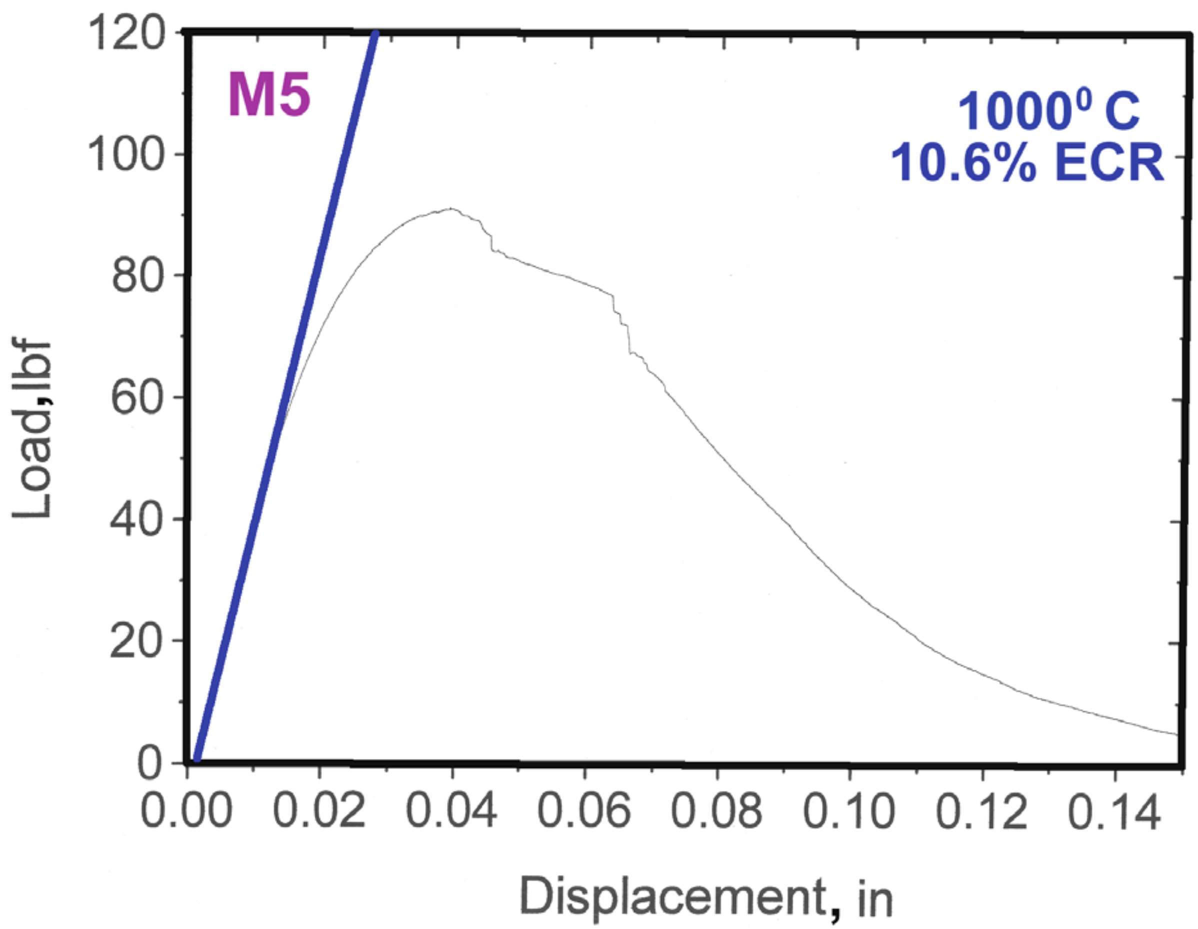

Fig. C.4 Ring-compression load-displacement data for M5 oxidized to ≈11% ECR at 1000˚C. Specimen compressed to within 3 mm of ID contact at 0˚ and 180˚ locations. Through-wall cracks at 0˚ and 180˚ in buckled region. Gradual load decrease appears to be due to effects of buckling of the prior-beta region at 0˚ and 180˚. Small additional hand compression caused failure at 90˚ and 270˚. Offset displacement is estimated to be 3.76 mm (0.15"), but first through-wall crack may have occurred at lower offset displacement.

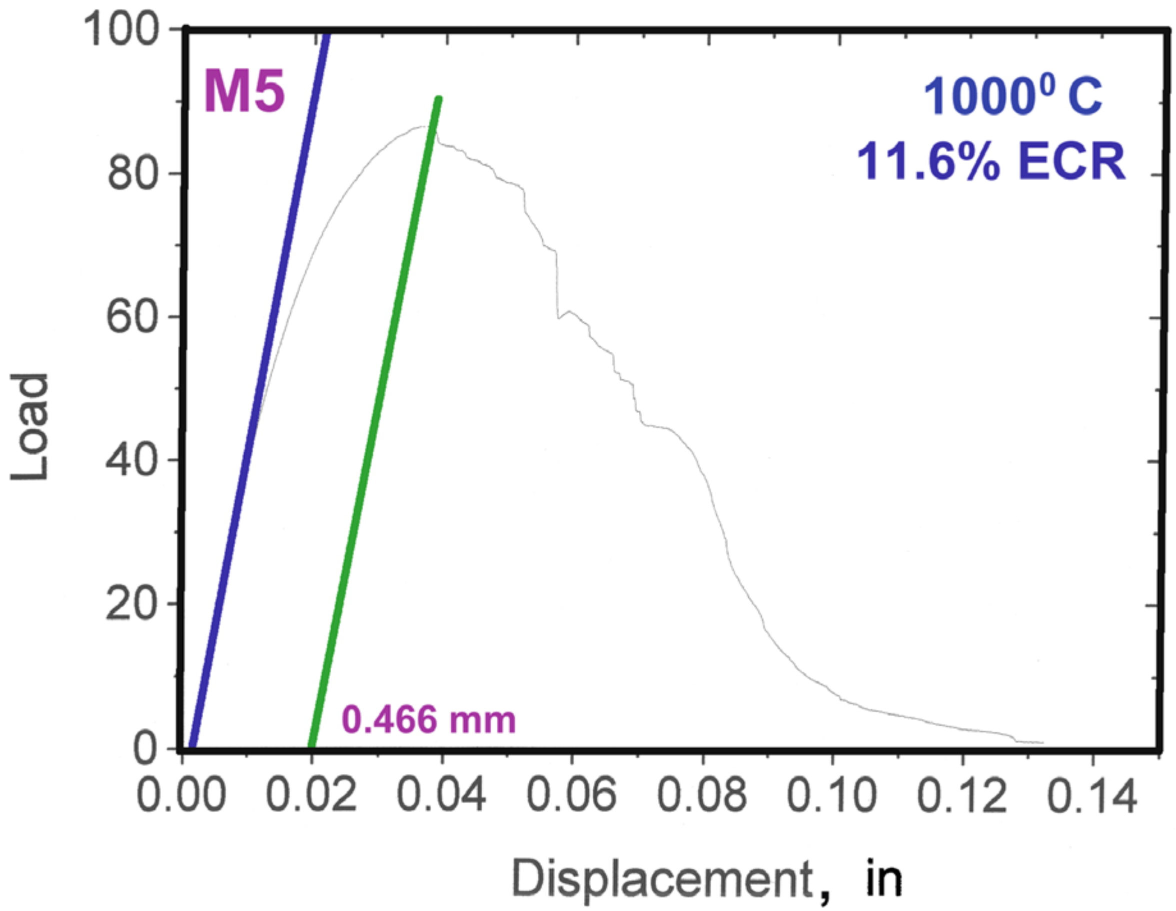

Fig. C.5. Ring-compression load-displacement data for M5 oxidized to ≈12% ECR at 1000˚C. Sample fractured into 3 pieces. Buckling is mild. It appears that through-wall cracks initiated at 0˚ and 180˚ first. This was confirmed in a separate test that was limited ≈2 mm (≈0.08") total displacement. Top and bottom surfaces were nearly flat. One through-wall crack observed at 0˚ or 180˚. Oxide/alpha crack at other top or bottom surface. Second test confirms that through-wall crack develops first at flattened top and/or bottom surface, before significant buckling. Offset displacement of ≤1.82 mm is based on this second test. Green line at 0.466-mm offset displacement is a reference line and was not used to determine offset strain.

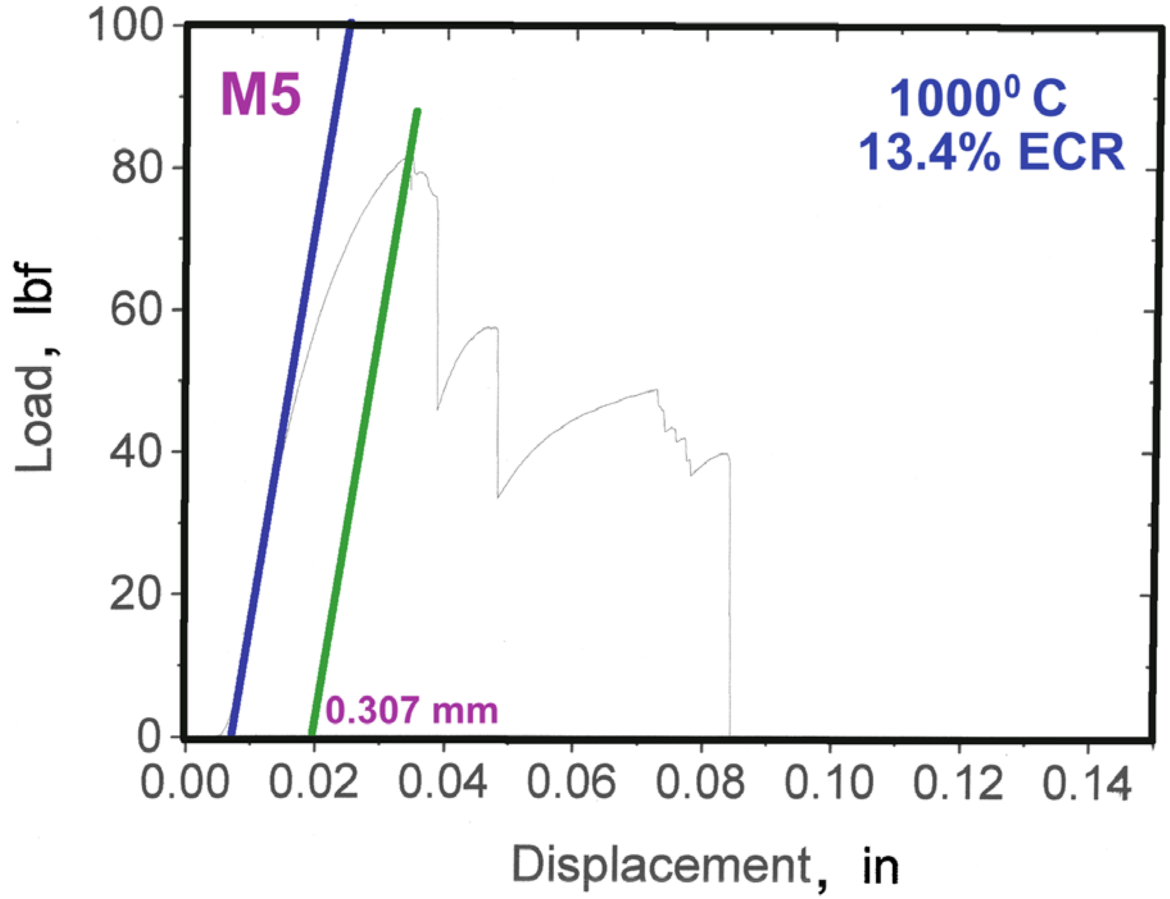

Fig. C.6. Ring-compression load-displacement data for M5 oxidized to ≈13% ECR at 1000˚C. Sample fractured into 4 pieces. The indicated offset displacement of 0.307 mm is a lower bound. Some additional plastic flow may have occurred between 0.31 mm and 0.45 mm that is obscured by the small cracks developing in the oxide/alpha regions prior to through-wall failure.

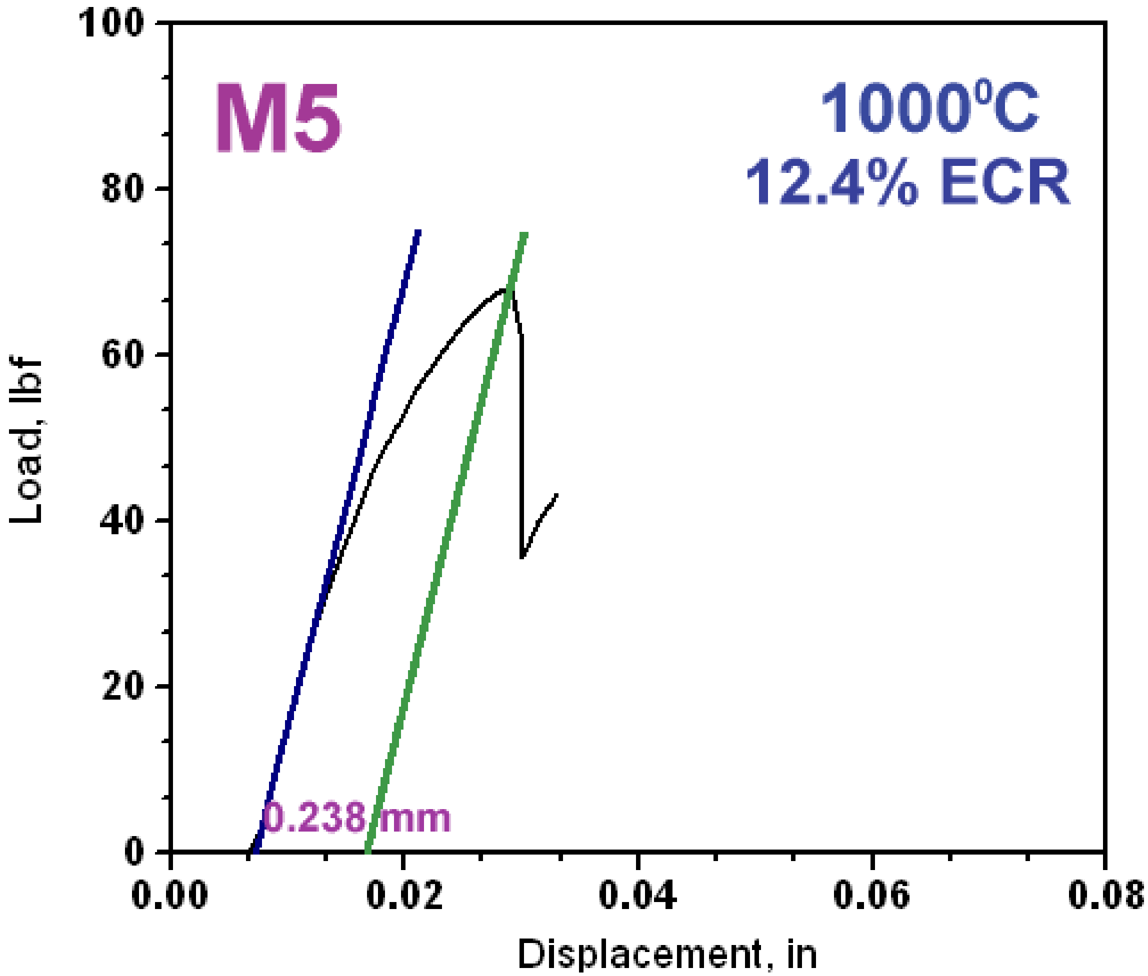

Fig. C.7 Ring-compression load-displacement data for M5 oxidized to ≈12% ECR at 1000˚C. The test was stopped after the first significant load drop, which led to a single through-wall crack at the support location. Offset displacement is 0.238 mm, while direct post-test measurements indicate 0.20 mm decrease in diameter along loading direction and 0.11 mm increase in diameter 90˚ from loading direction.

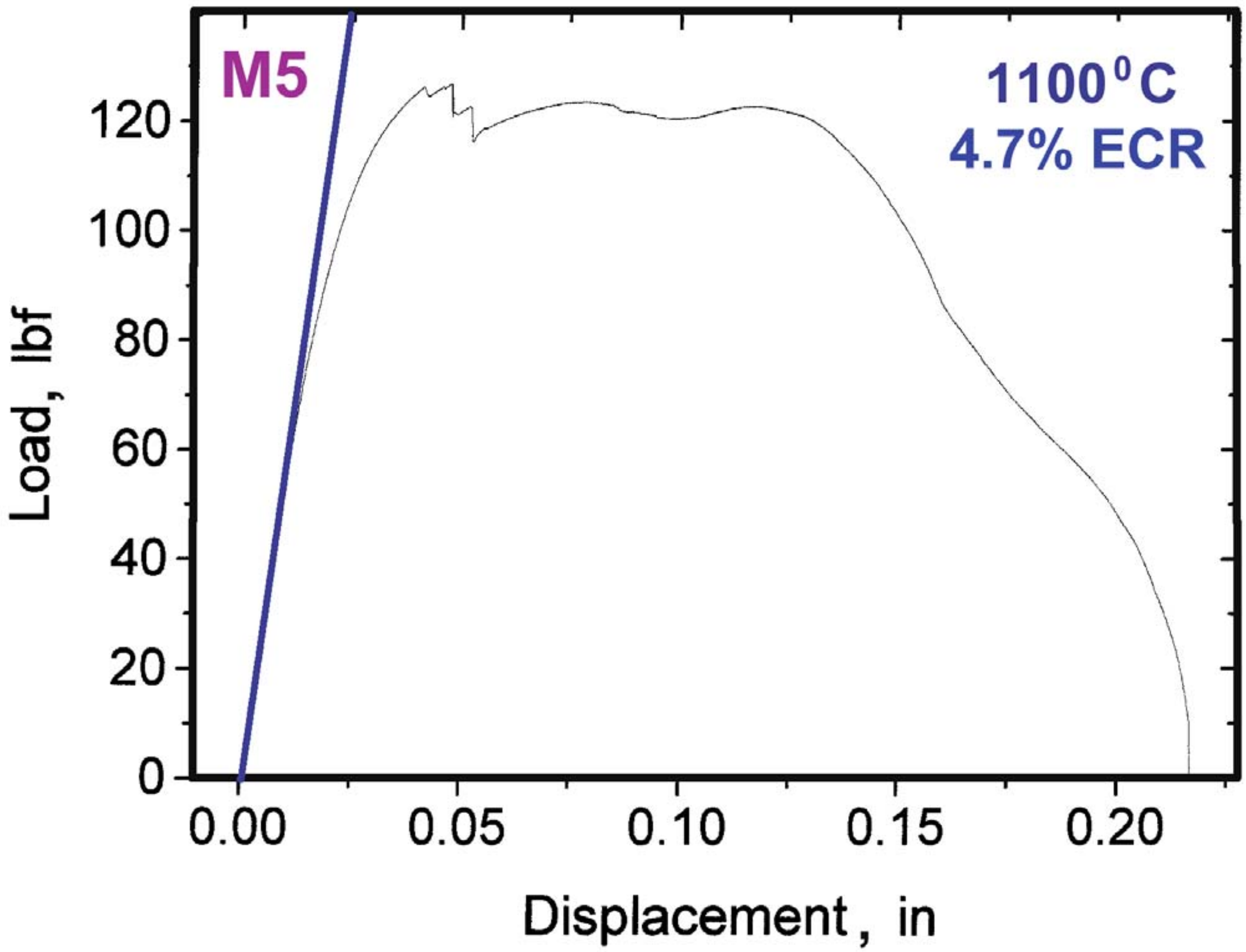

Fig. C.8 Ring-compression load-displacement data for M5 oxidized to ≈5% ECR at 1100˚C. Through-wall cracks observed at 0˚ and 90˚, most likely after significant deformation and buckling (see Fig. 12b). Offset displacement is estimated to be 5.4 mm (0.21").

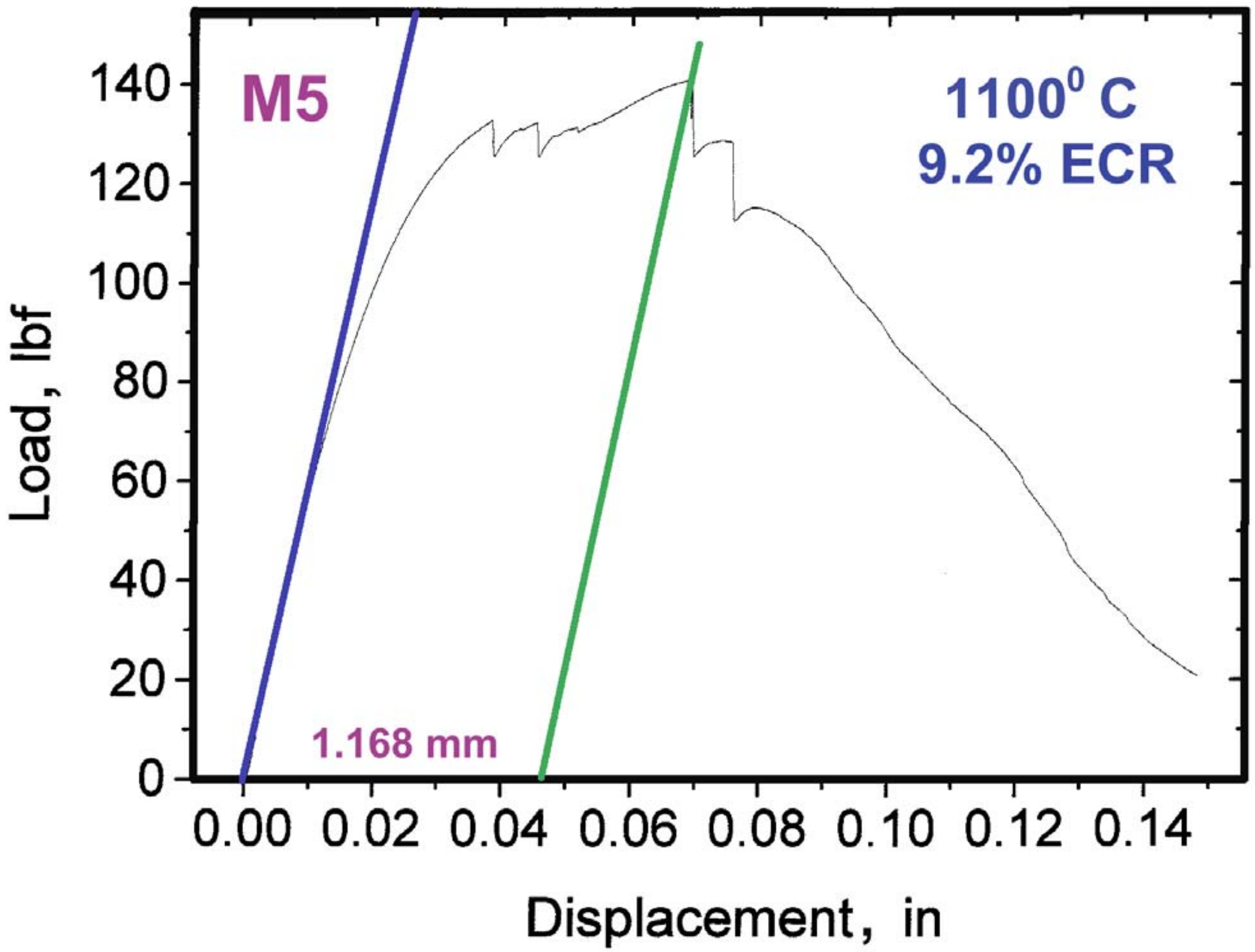

Fig. C.9 Ring-compression load-displacement data for M5 oxidized to ≈9% ECR at 1100˚C. No through-wall cracks observed. Significant buckling occurred. Green line at 1.168 mm indicates initiation of significant oxide/alpha cracking, but it does not indicate initiation of a through-wall crack.

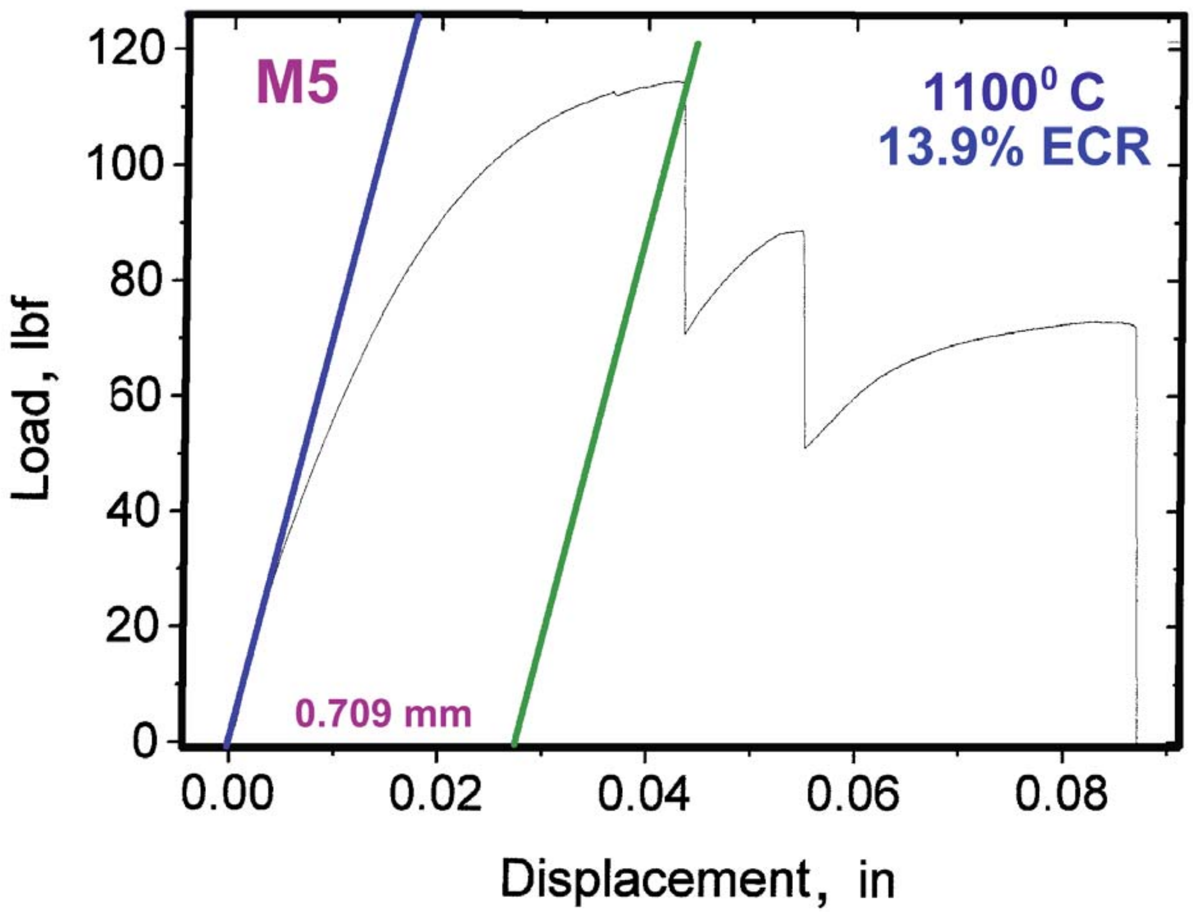

Fig. C.10 Ring-compression load-displacement data for M5 oxidized to ≈14% ECR at 1100˚C. Sample fractured into four pieces. Last load drop most likely represents formation of 2 through-wall cracks.

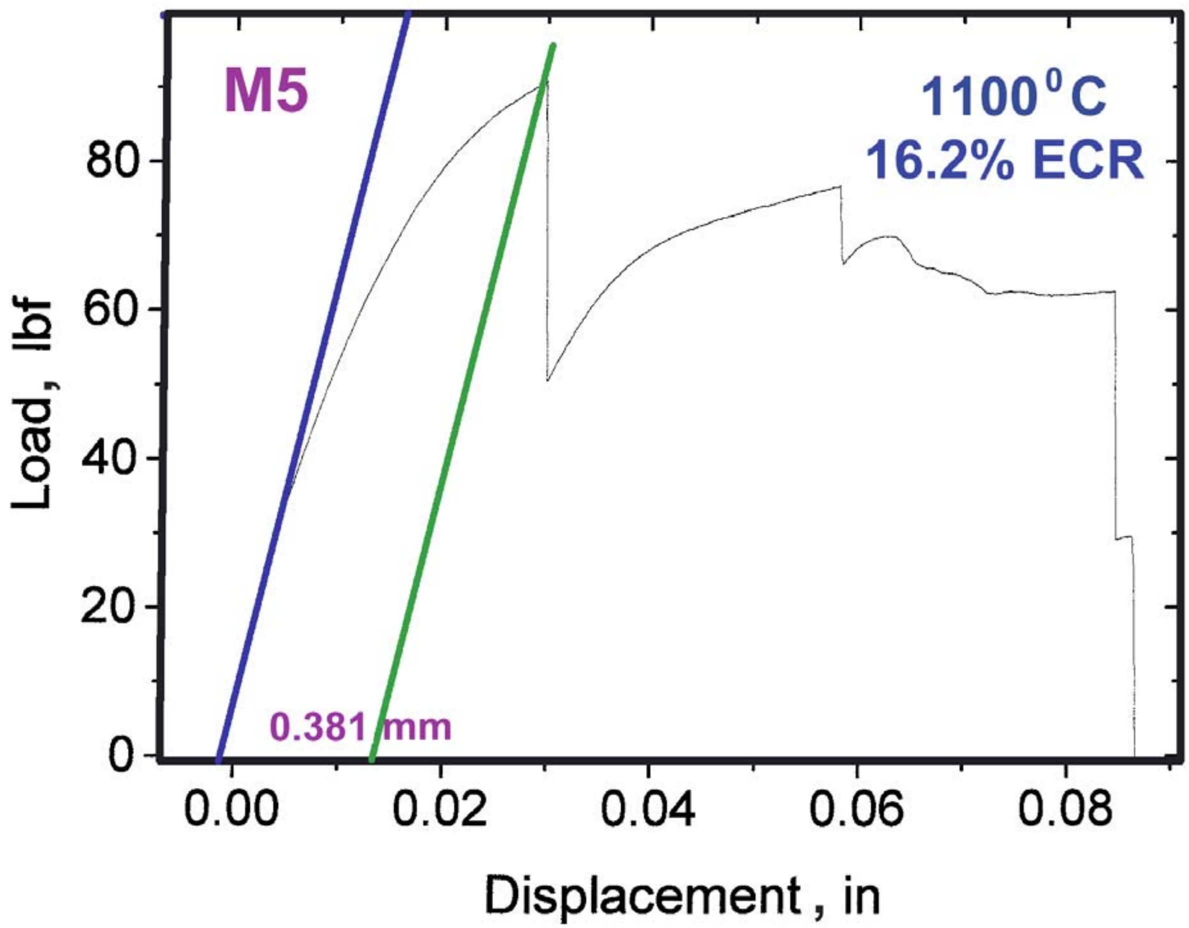

Fig. C.11 Ring-compression load-displacement data for M5 oxidized to ≈16% ECR at 1100˚C. Sample fractured into 4 pieces, with no buckling observed.

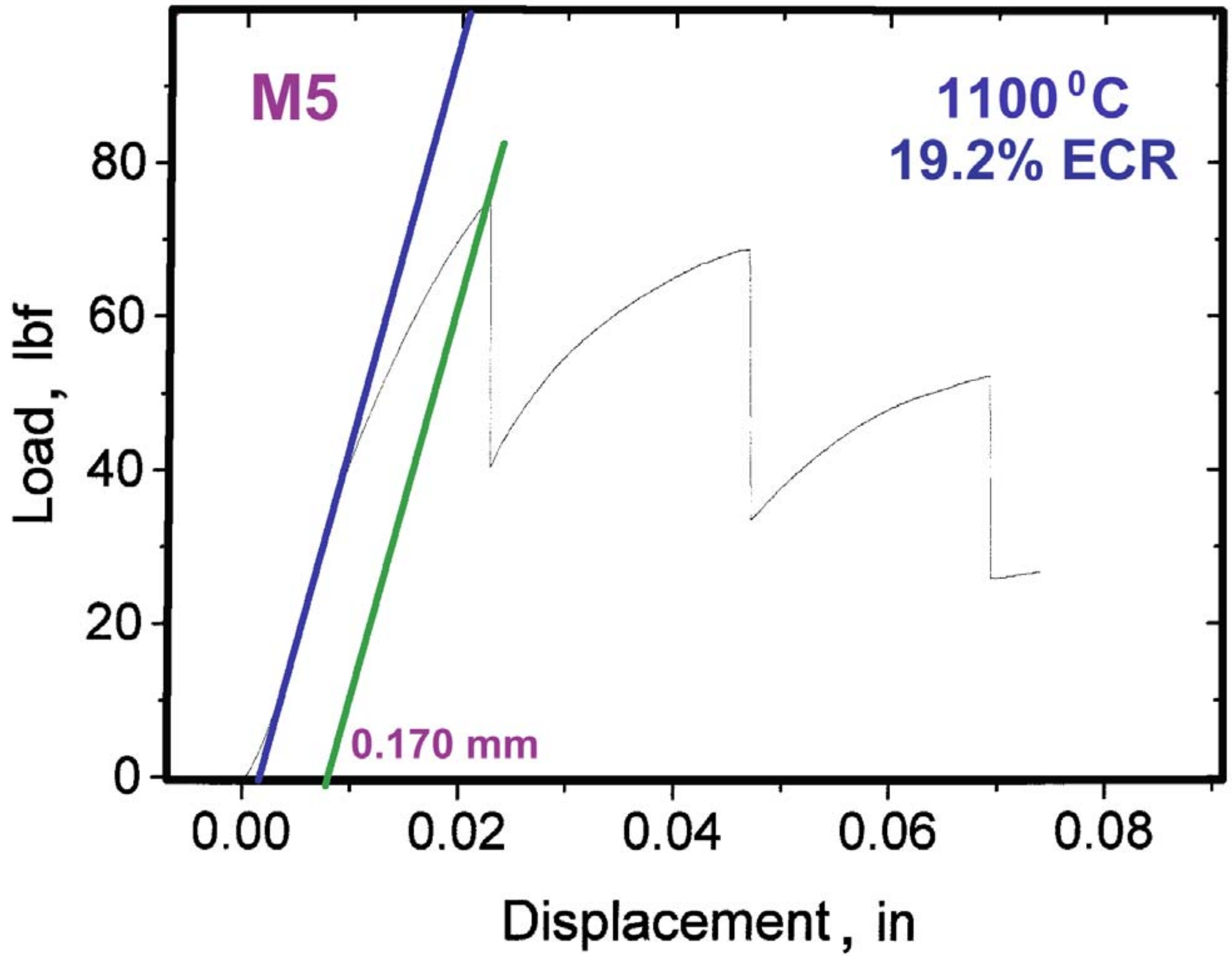

Fig. C.12 Ring-compression load-displacement data for M5 oxidized to ≈19% ECR at 1100°C. Sample fractured into three pieces, with the first through-wall failure occurring at very low offset displacement.

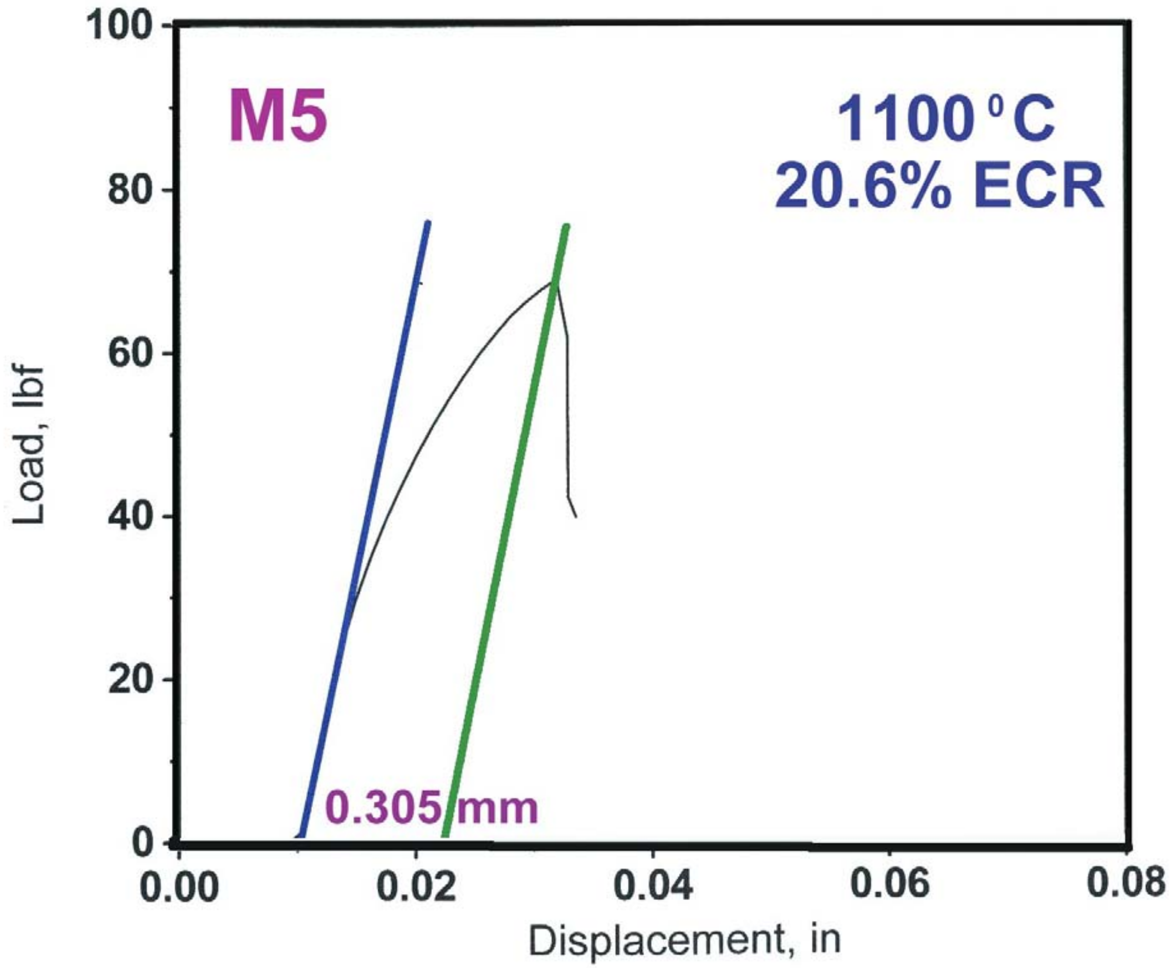

Fig. C.13 Ring-compression load-displacement data for M5 oxidized to ≈21% ECR at 1100˚C. The test was stopped after the first significant load drop, which led to a single through-wall crack at the support location. Offset displacement is 0.305 mm as compared to post-test-measured decrease in diameter of 0.11 mm along loading direction and increase in diameter of 0.08 mm 90˚ from loading line.